

**Parallelizing the Browser: Synthesis and Optimization of Parallel Tree
Traversals**

by

Leo A. Meyerovich

A dissertation submitted in partial satisfaction of the

requirements for the degree of

Doctor of Philosophy

in

Electrical Engineering and Computer Science

in the

Graduate Division

of the

University of California, Berkeley

Committee in charge:

Professor Rastislav Bodik, Chair

Professor George Necula

Professor Krste Asanovic

Professor David Wessel

Fall 2013

The dissertation of Leo A. Meyerovich, titled Parallelizing the Browser: Synthesis and Optimization of Parallel Tree Traversals, is approved:

Chair _____

Date _____

University of California, Berkeley

**Parallelizing the Browser: Synthesis and Optimization of Parallel Tree
Traversals**

Copyright 2013
by
Leo A. Meyerovich

Abstract

Parallelizing the Browser: Synthesis and Optimization of Parallel Tree Traversals

by

Leo A. Meyerovich

Doctor of Philosophy in Electrical Engineering and Computer Science

University of California, Berkeley

Professor Rastislav Bodik, Chair

From low-power phones to speed-hungry data visualizations, web browsers need a performance boost. Parallelization is an attractive opportunity because commodity client devices already feature multicore, subword-SIMD, and GPU hardware. However, a typical webpage will not strongly benefit from modern hardware because browsers were only designed for sequential execution. We therefore need to redesign browsers to be parallel. This thesis focuses on a browser component that we found to be particularly challenging to implement: the layout engine.

We address layout engine implementation by identifying its surprising connection with attribute grammars and then solving key ensuing challenges:

1. We show how layout engines, both for documents and data visualization, can often be functionally specified in our extended form of attribute grammars.
2. We introduce a synthesizer that automatically schedules an attribute grammar as a composition of parallel tree traversals. Notably, our synthesizer is fast, simple to extend, and finds schedules that assist aggressive code generation.
3. We make editing parallel code safe by introducing a simple programming construct for partial behavioral specification: schedule sketching.
4. We optimize tree traversals for SIMD, MIMD, and GPU architectures at tree load time through novel optimizations for data representation and task scheduling.

Put together, we generated a parallel CSS document layout engine that can mostly render complex sites such as Wikipedia. Furthermore, we scripted data visualizations that support interacting with over 100,000 data points in real time.

To You

Hey you! out there in the cold Getting lonely, getting old, can you feel me Hey you!
Standing in the aisles With itchy feet and fading smiles, can you feel me Hey you! don't
help them to bury the live Don't give in without a fight.

Contents

Contents	ii
List of Figures	iv
List of Tables	vii
1 Introduction	1
1.1 Mechanizing Layout Languages with Sugared Attribute Grammars	1
1.2 A Scheduling Language for Structuring and Verifying Parallel Traversals	1
1.3 Controlling Automatic Parallelization through Schedule Sketches	1
1.4 The Design of a Parallel Schedule Synthesizer	1
1.5 Optimizing Parallel Tree Traversals for Commodity Architectures	1
1.6 Collaborators and Publications	1
2 Layout Languages as Sugared Attribute Grammars	2
2.1 Motivation and Approach	2
2.2 Background: Layout with Classical Attribute Grammar	4
2.3 Desugaring Loops and Other Modern Constructs	8
2.4 Evaluation: Mechanized Layout Features	16
2.5 Related Work	17
3 A Safe Scheduling Language for Structured Parallel Traversals	18
3.1 Motivation and Approach	18
3.2 Background: Static Sequential and Task Parallel Visitors	18
3.3 Structured Parallelism in Visitors	18
3.4 A Behavioral Specification Language	19
3.5 Schedule Compilation	19
3.6 Schedule Verification	19
3.7 Automatically Staging Memory Allocation for SIMD Rendering	19
3.8 Scheduling Loops	24
3.9 Evaluation: Layout as Structured Parallel Visits	24
3.10 Related Work	25

4 Interacting with Automatic Parallelizers through Schedule Sketching	26
4.1 Automatic Parallelization: The Good, the Bad, and the Ugly	26
4.2 Holes	26
4.3 Generalizing Holes to Unification	26
4.4 Case Studies: Sketching in Action	26
4.5 Related Work	27
5 Parallel Schedule Synthesis	28
5.1 Motivation: Fast and Parameterized Algorithm Design	28
5.2 Optimized Algorithm: Finding One Schedule	28
5.3 Optimized Algorithm: Autotuning Over Many Schedules	28
5.4 Complexity Analysis and the Power of Sketching	28
5.5 Evaluation	28
6 Optimizing Tree Traversals for MIMD and SIMD	29
6.1 Overview	29
6.2 MIMD: Semi-static work stealing	30
6.3 SIMD Background: Level-Synchronous Breadth-First Tree Traversal	36
6.4 Input-dependent Clustering for SIMD Evaluation	38
6.5 Evaluation	42
6.6 Related Work	50
7 Conclusion	52
A Layout Grammars	53

List of Figures

2.1	Layout engine architecture.	4
2.2	For a language of horizontal boxes: (a) input tree to solve and (b) attribute grammar specifying the layout language. Specification language of attribute grammars shown in (c).	5
2.3	Dynamic data dependencies and evaluation. Shown for constraint tree in Figure ZZZ (a). Circles denote attributes, with black circles denote attributes with resolved dependencies such as input()s. Thin lines show data dependencies and thick lines show production derivations. Second chart shows the dependency graph resulting from evaluating all source nodes and marking them as resolved.	6
2.4	Dynamic attribute grammar evaluator. It selects attributes in a safe order by dynamically removing dependency edges as they are resolved.	7
2.5	Interfaces for tree grammars. Subfigures show manually encoding multiple production right-hand sides, an encoding that uses a Box non-terminal for indirection, and the high-level encoding using interfaces and classes.	9
2.6	Input tree as graph with labeled nodes and edges. Specified in the JSON notation.	10
2.7	Input tree as graph with labeled nodes and edges. Specified in the JSON notation.	11
2.8	Trait construct. Adds shared rendering code to the HBox class.	12
2.9	Input tree as graph with labeled nodes and edges. Specified in the JSON notation.	12
2.10	Visualization screenshots. All except [[CITE]] are interactive or animated. Each one was declaratively specified with our extended form of attribute grammars and automatically parallelized. Labels describe whether GPU or multicore code generation was used.	14
2.11	Document layout screenshots.	15
3.1	Partitioning of a library function that uses dynamic memory allocation into parallelizable stages.	20
3.2	Use of dynamic memory allocation in a grammar for rendering two circles.	21

3.3	Staged parallel memory allocation as two tree traversals. First pass is parallel bottom-up traversal computing the sum of allocation requests and the second pass is a parallel top-down traversal computing buffer indices. Lines with arrows indicate dynamic data dependencies.	22
6.1	Two representations of the same tree: naive pointer-based and optimized. The optimized version employs packing, breadth-first layout, and pointer compression via relative indexing.	30
6.2	Simulation of work stealing. Top-down simulated tree traversal of a tiled tree by three processors in three steps.	32
6.3	Simulation of work stealing on Wikipedia. Colors depict claiming processor and dotted boundaries indicate subtree steals. Top-left boxes measure hit rate for individual processor.	33
6.4	Temporal cache misses for simulated work stealing over multiple traversals. Simulation of 4 threads on Wikipedia. Blue shade represents a hit and red a miss. 67% of the nodes were misses. Top-left boxes measure hit rate for individual processor.	34
6.5	Dynamic work stealing for three traversals. Tiles are claimed by different processors in different traversals.	35
6.6	Semi-static work stealing. Dynamic schedule for first traversal is reused for subsequent ones.	35
6.7	SIMD tree traversal as level-synchronous breadth-first iteration with corresponding structure-split data representation.	37
6.8	blah	39
6.9	ASDF.	40
6.10	Loop transformations to exploit clustering for vectorization.	41
6.11	Sequential and Parallel Benefits of Breadth-First Layout and Staged Allocation. Allocation is merged into the 4th stage and buffer indexing and tessellation form the rendering pass. JavaScript variants use HTML5 canvas drawing primitives while WebCL does not include WebGL painting time (< 5ms). Thin vertical bars indicate standard deviation and horizontal bars show deadlines for animation and hand-eye interaction.	44
6.12	Multicore vs. GPU Acceleration of Layout. Benchmark on an early version of the treemap visualization and does not include rendering pass.	46
6.13	Compression ratio for different CSS clusterings. Bars depict compression ratio (number of clusters over number of nodes). Recursive clustering is for the reduce pattern, level-only for the map pattern. ID is an identifier set by the C3 browser for nodes sharing the same style parse information while value is by clustering on actual style field values.	47
6.14	Speedups from clustering on webpage layout. Run on a 2.66GHz Intel Core i7 (GCC 4.5.3 with flags -O3 -combine -msse4.2) and does not preprocessing time.	48
6.15	Performance/Watt increase for clustered webpage layout.	49

6.16 **Impact of data relayout time on total CSS speedup.** Bars depict layout pass times. Speedup lines show the impact of including clustering preprocessing time.

List of Tables

3.1	Lines of Code Before/After Invoking the '@' Macro	24
6.1	Speedups and strong scaling across different backends (Back) and hardware. Baseline is a sequential traversal with no data layout optimizations. FTL is our multicore tree traversal library. Left columns show total speedup (including data layout optimizations by our code generator) and right columns show just parallel speedup. Server = Opteron 2356, laptop = Intel Core i7, mobile = Atom 330.	43
6.2	Parallel CSS layout engine. Run on a 2356 Opteron.	43

Acknowledgments

I want to thank my advisor for advising me.

Chapter 1

Introduction

Why Parallel Computing

Why Mechanize Layout

Approach

- 1.1 Mechanizing Layout Languages with Sugared Attribute Grammars
- 1.2 A Scheduling Language for Structuring and Verifying Parallel Traversals
- 1.3 Controlling Automatic Parallelization through Schedule Sketches
- 1.4 The Design of a Parallel Schedule Synthesizer
- 1.5 Optimizing Parallel Tree Traversals for Commodity Architectures
- 1.6 Collaborators and Publications

Chapter 2

Layout Languages as Sugared Attribute Grammars

2.1 Motivation and Approach

We start by examining challenges for building layout languages and our high-level solution of automation through attribute grammars. Throughout this and the remaining chapters, we focus on the design and implementation of one simple layout widget. We will show how our support of it generalizes to common layout languages and, more generally, computations over trees.

Important properties for layout languages and others

Layout languages are some of the most common – for one gauge, there are over 634 million websites live in 2012, with 51 million added that year¹. Beyond the CSS and HTML languages used for webpage layout, designers also use LATEX [[CITE]] for document layout, D3 [[CITE]] for data visualization, Swing [[Swing]] for GUI layout, and even specialize within these domains such as by using markdown for text.

Popular layout languages foster designer productivity by providing abstractions that are rich and numerous. The alternative is analogous to asking a programmer to write in a low-level language such as assembly: designers should not manually specify, for each element, the position on a canvas and the style. Instead, layout languages resemble constraint systems where designers declare high-level properties. For example, the high-level program `hello world` states that the words `hello` and `world` should be rendered, and word `world` should follow line-wrapping rules for its positioning after `hello`. Layout languages may provide quite complicated constraints – for example, most document layout languages resort to defining their line wrapping rule in a flexible low-level language. Likewise, they may provide many features, such as in the 250+ pages of rules for the CSS language. Adding to the sophistication, many

¹<http://news.netcraft.com/archives/2012/12/04/december-2012-web-server-survey.html>

languages support designers adding their own constraints, such as through macros in L^AT_EX, percentage constraints in CSS, and arbitrary functions in Adobe Flex [[CITE]].

The richness of popular layout languages comes at the cost of complicating their design and implementation:

- **Safe semantics.** Does every input layout have exactly one unique rendering? Are the constraints restricted enough such that an efficient implementation is feasible for low-power devices, big data sets, and fast animation? When a feature is added, does it conflict with anything of the above properties? We want an automated way to verify such properties.
- **Safe implementation.** As a layout language grows in popularity, it grows in features. Likewise, developers will port it to many platforms and optimize it, and in cases such as CSS, reimplement it from scratch. Does the implementation conform to the intended semantics? Conformance bugs for CSS plague developers [[CITE]], and failures to match L^AT_EX’s semantics have killed multiple attempts to modernize the implementation. We want an automated way to ensure that the implementation matches the specification.
- **Advanced implementation.** Layout languages tend to add feature as they evolve. However, the implementation of each feature also has demands that increase with time: improved speed and memory footprint, better debugging support, etc. Browser layout engines for CSS are currently over 100,000 lines of optimized C++ code, and most rich layout languages thus far have resisted parallelization. We want automation techniques to lower the implementation burden and more aggressively target those goals.

Our idea is to declaratively specify layout languages and automatically compile them into an efficient implementation. At runtime, an instance of layout will be processed through the previously generated layout engine (Figure 2.1). The compiler is responsible for checking the semantics of the layout features and, by construction, provides a correct implementation. Furthermore, instead of manually optimizing the code for every individual feature, language designers instead write generic compiler optimizations. As a similar implementation benefit, we automatically target multiple platforms for the same layout language, such as scripting languages in order to use their debuggers, and multicore and GPU languages to gain magnitudes of speedups.

We show that the attribute grammar formalism supports specification of layout languages. It is unclear how to encode complicated layout language features with the traditional formalism, so we support a rich form of attribute grammars and reduce reasoning about them to handling a more traditional formalism (reducer in Figure 2.1). The remainder of this chapter introduces the high-level attribute grammar formalism, how to specify layout languages using it, and an intuition for the reduction into a lower-level formalism.

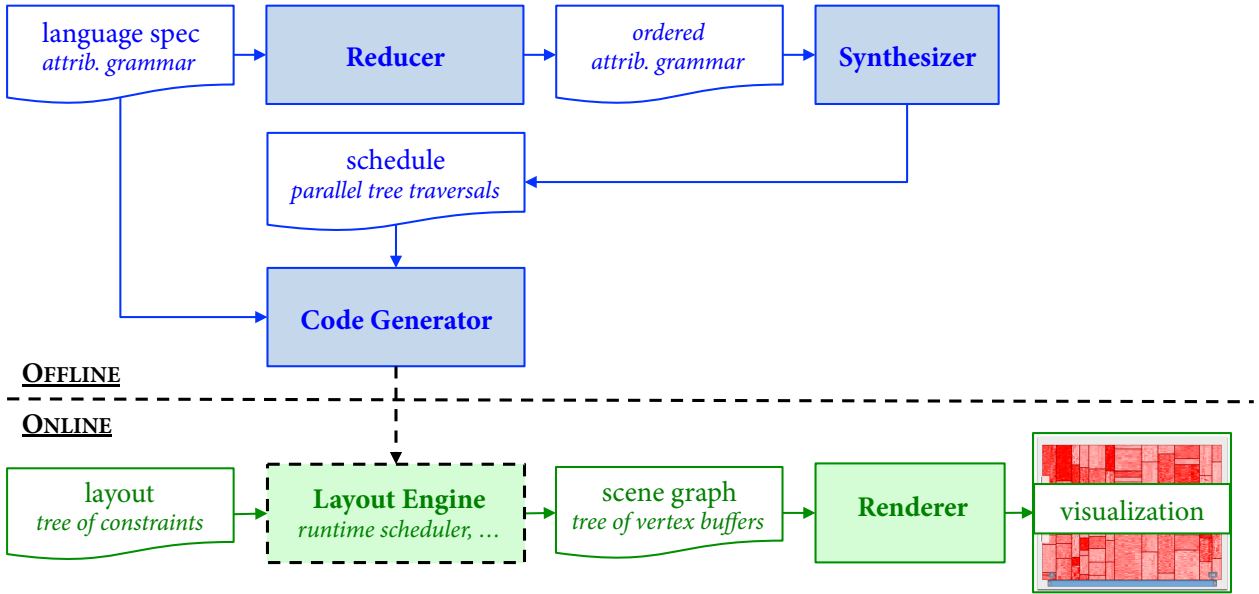


Figure 2.1: Layout engine architecture.

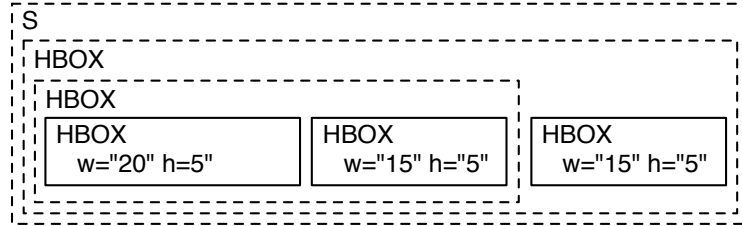
2.2 Background: Layout with Classical Attribute Grammar

This section describes specifying a simple layout language as an attribute grammar and two classical implementation strategies. We reuse the example throughout our work to explore various concepts.

Attribute Grammars

Consider solving the tree of horizontal boxes shown in Figure 2.2 (a). As input, a webpage author provides a tree with constraints (Figure 2.2 ??). Only some node attribute values are provided: in this case, only the widths and heights of leaf nodes. The meaning of a horizontal layout is that, as is visualized, the boxes will be placed side-by-side. The layout engine must solve for all remaining x, y, width, and height attributes.

We declaratively specify the layout language of horizontal boxes, H-AG, as shown in Figure 2.2 (c), with an attribute grammar [oag, Meyerovich:2010, htmlag]. First, the specification defines the set of well-formed input trees as the derivations of a context-free grammar. We use the standard notation [[CITE]]. In this case, a document is an unbalanced binary tree of arbitrary depth where the root node has label **S** and intermediate nodes have label **HBOX**. Second, the specification defines semantic functions that relate attributes associated with each node. For example, the width of an intermediate horizontal node is the sum of its children widths. Likewise, the width of a leaf node is provided by the user, which is encoded by the nullary function call *input_w*():

(a) **Input tree.** Only some of the x, y, w, and h attributes are specified.

```

<S>
  <HBox name=child>
    <HBox name=left >
      <HBox name=left w=20 h=5/>
      <HBox name=right w=15 h=5/>
    </HBox>
    <HBox name=right w=15 h=5/>
  </HBox>
</S>

```

(b) **Textual encoding of input tree.**

$$S \rightarrow HBOX$$

$$\{ HBOX.x = 0; HBOX.y = 0 \}$$

$$HBOX \rightarrow \epsilon$$

$$\{ HBOX.w = \text{input}_w(); HBOX.h = \text{input}_h() \}$$

$$HBOX_0 \rightarrow HBOX_1 \ HBOX_2$$

$$\{ HBOX_1.x = HBOX_0.x;$$

$$HBOX_2.x = HBOX_0.x + HBOX_1.w;$$

$$HBOX_1.y = HBOX_0.y;$$

$$HBOX_2.y = HBOX_0.y;$$

$$HBOX_0.h = \max(HBOX_1.h, HBOX_2.h);$$

$$HBOX_0.w = HBOX_1.w + HBOX_2.w \}$$
(c) **Attribute grammar for a language of horizontal boxes.**

$$AG \rightarrow (\text{Prod } \{ \text{Stmnt?} \})^*$$

$$\text{Prod} \rightarrow V \rightarrow V^*$$

$$\text{Stmnt} \rightarrow \text{Attrib} = id(\text{Attrib}^*) \mid \text{Attrib} = n \mid \text{Stmnt} ; \text{Stmnt}$$

$$\text{Attrib} \rightarrow id.id$$
(d) **Language of attribute grammars.**

Figure 2.2: For a language of horizontal boxes: (a) input tree to solve and (b) attribute grammar specifying the layout language. Specification language of attribute grammars shown in (c).

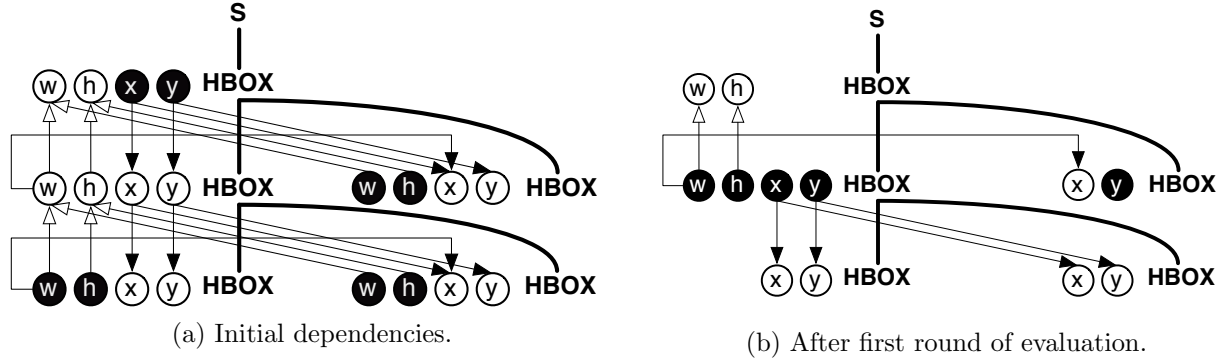


Figure 2.3: **Dynamic data dependencies and evaluation.** Shown for constraint tree in Figure ZZZ (a). Circles denote attributes, with black circles denote attributes with resolved dependencies such as `input()`s. Thin lines show data dependencies and thick lines show production derivations. Second chart shows the dependency graph resulting from evaluating all source nodes and marking them as resolved.

$$\begin{aligned}
 HBOX &\rightarrow \epsilon \{ \text{HBOX}.w = \text{input}_w(); \dots \} && /* \text{leaf} */ \\
 HBOX_0 &\rightarrow HBOX_1 \text{ HBOX}_2 && /* \text{binary node} */ \\
 &\{ \dots \text{HBOX}_0.w = \text{HBOX}_1.w + \text{HBOX}_2.w \}
 \end{aligned}$$

The specification intentionally does not define the evaluation order. For example, the specification does not state whether to compute a node's width before its height. Likewise, our optimized approach will compute the attributes as a sequence of tree traversals, but the specification does not state what those traversals are. Leaving the evaluation order unspecified provides freedom for our compilers to pick an efficient parallel order. Irrespective of whatever evaluation order is ultimately used to solve for the attribute values, the statements define constraints that must hold over the computed result. Attribute grammars can therefore be thought of as a single assignment language where attributes are dataflow variables [[CITE]].

The language of attribute grammars is defined in Figure 2.2 (d). In addition to defining the context free grammar, it supports single-assignment constraints over attributes of nodes in a production. Our example uses the following encoding. Semantic functions are pure and left uninterpreted, so, for example, we encode the addition of widths as “ $\text{HBOX}_0.w = f(\text{HBOX}_1.w, \text{HBOX}_2.w)$ ”. Our program analysis techniques do not need to know the contents of the function, just that the output of a call depends purely on the inputs. For the same reason, we encode constant values as nullary function calls.

To specify grammars more complicated than **H-AG**, we describe linguistic extensions for richer functional specifications (Section 2.3) and, to control the evaluation order, behavioral specification (Chapters 3 and 4).

```

input:  $G = (V, E)$ 
output:  $Map$ 
 $Map \leftarrow \emptyset$ 
 $E' \leftarrow E$ 
 $V' \leftarrow V$ 
for  $a \in V'$  where  $\exists(n, a) \in E'$ :
     $Map \leftarrow Map \cup \{a \rightarrow \text{eval}(a)\}$ 
     $V' \leftarrow V' - a$ 
     $E' \leftarrow E' (\{a\} \times V)$ 
repeat until  $E' = \emptyset$ 
return  $Map$ 

```

Figure 2.4: **Dynamic attribute grammar evaluator.** It selects attributes in a safe order by dynamically removing dependency edges as they are resolved.

Dynamic data dependencies and dynamic evaluation

A simple and classic evaluation strategy is to *dynamically* compute over a tree. The evaluator dynamically follows the dynamic data dependencies between instances of attributes. The dynamic evaluation strategy is too slow for our use cases, but it introduces the key concepts of dynamic data dependencies, the dynamic semantics of attributes grammars, and the corresponding dynamic interpreter.

An instance of a document corresponds to the dependency graph shown in Figure ?? (a). Each attribute of a tree node is either a source, meaning its value can be computed based on other known values, or it cannot be evaluated until other attribute values are known. It is a dynamic dependency graph in that each data dependency in the static code may be instantiated as multiple data dependencies given a tree at runtime.

The dynamic data dependency graph leads to a simple semantics for the result of evaluation. The graph corresponds to a system of equations where edges link instance variables. For example, static code `HBOX$._2$.x = HBOX$._0$.x + HBOX$._1$.w` instantiates twice for the Figure 2.3 ??: once for each x attribute with an incoming elbow connector. The value of both xs are constrained by distinct instances of the above constraint. If the dependency graph is a directed acyclic graph and each attribute appears on the lefthand side of exactly one equality statement (*dataflow variables*), there is exactly one solution to the system of equations.

A simple procedure solves an instance of a system of equations: topological traversal. The algorithm is as follows: The algorithm literately finds an attribute whose dependencies have all been previously resolved, evaluates the attribute, and repeats. If the input graph is a directed acyclic graph, this procedure is guaranteed to terminate. The insight is that a directed acyclic graph has at least one fringe node, the loop removes them, and removing these nodes yields a smaller directed acyclic graph.

The dynamic evaluation strategy provides a small explanation for the natural semantics, but it leaves several challenges. First, runtime manipulation of a dynamic dependency graph introduces high overheads because every dynamic dependency edge must be manipulated.

Second, it is unsafe. For example, a cycle in the dependency graph causes the above evaluation strategy to get stuck, so dynamic evaluators must introduce runtime cycle check. Designers can build layout widgets that, depending on how they are invoked, fail to display!

2.3 Desugaring Loops and Other Modern Constructs

The attribute grammar formalism was invented for describing semantics [[CITE]] and before many modern constructs became mainstream: we had to design extensions for improved expressiveness and maintainability. Our extensions exploit concepts from structured, object-oriented, and functional programming. Other language designers have built such extensions as well [[CITE]]: our challenge was to make expressive extensions that facilitate effective parallelization and do not overly complicate language and tool implementation. This section documents the language features and how they simplify implementation, and leaves performance optimization to the next chapter.

Our key insight is that pre- and post-processing supports desugaring a feature-rich attribute grammar into the canonical attribute grammar notation. Tools then operate at the most appropriate stage, such as our scheduler on the small, canonical attribute grammar representation. Likewise, our code generators take a generated schedule and relate it back to a representation from early in the preprocessing stage. Many of the below features are built as explicit compiler stages, but over time, we found that declarative tree rewriting systems such as ANTLR and OMeta support automating individual stages.

Interfaces for Encoding Tree Grammars

Attribute grammars are an extension to the tree grammar formalism for defining input trees, so improving the abstraction capabilities of tree grammars also aids the ability to structure attribute grammars. In particular, we found the need to support abstracting over similar types of non-terminals. Our solution is to provide a notion of classes and interfaces. Our core extension is macro-expressible with attribute grammars and therefore reduces implementation requirements, though it is still important enough that it merits deeper compiler support.

Consider the code duplication performed when extending H-AG with vertical boxes. The children of a HBox could be a horizontal box or a vertical box, and the same for the children of a vertical box. Figure ?? shows that the 3 productions of H-AG grew to be 11. The example highlights that canonical attribute grammars cannot abstract over node types. Adding a new box type requires modifying all previous box classes, and in the presence of multiple children, extension suffers exponential costs.

To abstract over node types, we introduce the notion of classes and interfaces (Figure 2.5b). Classes are similar to the productions of an attribute grammar: the class name specifies the production's lefthand side non-terminal and the children block specifies the production's righthand side. Unlike attribute grammars, an interface name is used for the

$S \rightarrow HBOX \mid VBOX$
 $HBOX \rightarrow \epsilon$
 $HBOX_0 \rightarrow HBOX_1 HBOX_2$
 $HBOX_0 \rightarrow VBOX_1 HBOX_2$
 $HBOX_0 \rightarrow HBOX_1 VBOX_2$
 $HBOX_0 \rightarrow VBOX_1 VBOX_2$
 $VBOX \rightarrow \epsilon$
 $VBOX_0 \rightarrow HBOX_1 HBOX_2$
 $VBOX_0 \rightarrow VBOX_1 HBOX_2$
 $VBOX_0 \rightarrow HBOX_1 VBOX_2$
 $VBOX_0 \rightarrow VBOX_1 VBOX_2$

(a) Canonical attribute grammar.

```

interface BoxI { }
class HBoxLeaf : BoxI { }
class HBoxBinary : BoxI {
    children {
        left: BoxI;
        right: BoxI;
    }
}
class VBoxLeaf : BoxI { }
class VBoxBinary : BoxI {
    children {
        left: Box;
        right: Box;
    }
}

```

(b) Interface sugar.

$S \rightarrow BOX$
 $BOX \rightarrow HBOX \mid VBOX$
 $HBOX \rightarrow \epsilon$
 $HBOX_0 \rightarrow BOX_1 BOX_2$
 $VBOX \rightarrow \epsilon$
 $VBOX_0 \rightarrow BOX_1 BOX_2$

(c) Interface encoding.

Figure 2.5: **Interfaces for tree grammars.** Subfigures show manually encoding multiple production right-hand sides, an encoding that uses a Box non-terminal for indirection, and the high-level encoding using interfaces and classes.

```
{
  "class": "HBox",
  "children": {
    "left": {
      "class": "HBox",
      "children": {
        "left": {"class": "HBox", "w": 20, "h": 5},
        "right": {"class": "HBox", "w": 15, "h": 5}
      }
    },
    "right": {"class": "HBox", "w": 15, "h": 5}
  }
}
```

Figure 2.6: **Input tree as graph with labeled nodes and edges.** Specified in the JSON notation.

righthand side rather than the class name. `HBox` and `VBox` implement interface `BoxI`, so any class specified to have a `BoxI` child can have a `HBox` or `VBox` child within the concrete tree.

Classes and interfaces are formally equivalent to tree grammars in the sense of a 1-to-1 correspondence between trees described by both. First, a tree grammar can be expressed with classes and interfaces by treating all productions with the same lefthand-side non-terminal as different classes belonging to the same interface. In the other direction, each interface can be expressed as a production that derives the classes, and the classes expand into productions. Figures 2.5b and 2.5c demonstrate the correspondence for `H-AG`. The induced implementation requirements are therefore slight in the sense that the construct is sugar for a pattern in the canonical attribute grammars.

We depart from the correspondence for the encoding of trees in two ways. First, we represent input as a tree with labeled nodes and edges. Node labels denote the class and edge labels specify child bindings. Figure 2.7 uses the JSON format common to dynamic languages for an instance of a tree in `H-AG`. By naming children, such as `left` and `right`, we eliminate sensitivity to their order within a code block. With order sensitivity, adding a middle child `center` would needlessly require refactoring references to the repositioned element `right`. Likewise, reordering children in the input data does not require refactoring the attribute grammar.

Our second departure from the canonical attribute grammar encoding optimizes the data representation by eliding intermediate interface nodes. The reduction to attribute grammars suggests adding a new non-terminal for each interface, but doing so in the data representation doubles the number of nodes in the concrete tree. Making the interface pattern a language construct with compiler support eliminates associated costs, such as cutting file size for runtime parsing of big data visualizations.

Interfaces for attributes and information hiding.

Our system provides lightweight specification annotations for different types of attributes, and coupled with the interface construct, it supports defining relationships between attributes across different classes.

```

interface BoxI {
    var x : float;
}
class HBoxLeaf : BoxI {
    attributes {
        var y : int;
        input w : ? int;
        input h : int = 10;
    }
}

```

Figure 2.7: Input tree as graph with labeled nodes and edges. Specified in the JSON notation.

Each static attribute is annotated with its assignment type and its embedded value type:

- **Assignment types.** The assignment type denotes whether the input tree defines the value, such as in `input w`, or whether the attribute grammar defines it, as in `var x`. Assignments to an input type are illegal, and multiple assignments to a variable type are also illegal.

If an input tree fails to provide an input attribute, a runtime error will be thrown. To still provide an interpretation of such trees, input attributes support the annotation "?", which enables pattern matching through functions `maybeReady :: -> boolean` and `maybeValue :: -> 'a`. Alternatively, for the common scenario of using a fixed default value, a default value can instead be defined as in `input h : int = 10`. If the input tree does not provide the value, the default value will be automatically substituted.

Canonical attribute grammars can encode input attributes in two ways. First, semantic functions with no parameters encode the lack of dependencies. Second, for finite domains, the set of tree grammar productions can expand to include attribute nodes. The second encoding more faithfully describes our approach because, like our system, it feeds into an automatic tree parser generator. For each tree node, our generated parser scans for the expected set of input attributes.

- **Value types.** The system also supports type annotations used for embeddings. Generated code typically compiles as part of a project in a more static language, such as C++, which require a static type discipline. The annotations can be user-defined, such as OpenGL's *vertex buffer object* VBO, which is not defined within our system.

Our analyzer ignores the value type annotations such as `x : float` and `y : int` while the low-level code generator passes along the decorations `float` and `int`. The embedded design simplifies implementation because value type checking is performed by the host language's compiler.

In practice, we use attribute definitions in interfaces for information hiding across classes and lightweight specification of relationships between similar classes. An attribute declared

```

trait Rectangle {
    attributes { render : int; }
    actions { render := paintRect(x,y,w,h, "black"); }
}
class HBox(Rectangle) : BoxI { ... }

```

Figure 2.8: **Trait construct.** Adds shared rendering code to the HBox class.

```

interface BoxI {
    var w : int;
    var h : int;
    var right : int;
    var bottom : int;
}
class HBox : BoxI {
    children {
        child : [ BoxI ]
    }
    actions {
        loop child {
            w := fold 0 .. self$ -w + child.w;
            h := fold 0 .. max(self$ -h, child.h)
            child.right := fold x .. child$ -right + child.w;
            child.bottom := fold y .. child$ -bottom + child.h;
        }
    }
}

```

Figure 2.9: **Input tree as graph with labeled nodes and edges.** Specified in the JSON notation.

inside of a class is *local* to constraints in the class: only the class's constraints can read or write to the attribute. Conversely, declaring a *var* inside of an interface hints that it is meant to be reused by outside classes, such as part of a tree traversal.

Traits: Reusing Cross-cutting Code

As with many object systems, we support a trait construct for cross-cutting code that should be shared across classes. It statically expands like a macro, and therefore provides no formal expressive power. For example, Figure 2.8 defines how to render a rectangle given several attributes, and then adds that functionality to class HBox. If the language was extended with class VBox, the class definition of VBox could also use trait Rectangle.

Loops

We extend our language with declarative loops over the attributes of multiple nodes. They are an expressive extension over the uniform recurrence relations of [[CITE]].

The loop construct, `loop`, specifies a block of loop body statements. It acts over a sequence of nodes declared with the same interface, such as `childs : [BoxI]` in Figure 2.9. The looping order is restricted to forward iteration, though our approach generalizes to other loop orders.

A statement in a loop body will execute for each element of the list. For example, the following statement assigns the attribute `w` the sum of the children widths: `w := fold 0 .. self$-.w + childs$i.w`. Similar to array index notation, the suffix on righthand-side variable names for loop statements provide a restricted form of relative indexing for loops. In particular:

- `$i`: the “current” loop step
- `$-`: the previous loop step
- `$$`: the last loop step

Use of suffix “`$-`” in a `fold` can be thought of as an accumulator in functional programming.

One loop statement can refer to the accumulator of another, which `fold` statements in most languages do not support. For example, two loop counters can be intertwined:

```
loop childs {
    childs.counter1 := fold 0 .. childs$-.counter2 + 1;
}
loop childs {
    childs.counter2 := fold 0 .. childs$-.counter1 + 1;
}
```

The programmer does not need to order the statements. For example, our system infers that the imperative code that implements the above declarations is just one imperative loop that fuses them together. The incorrect alternative of implementing the declarations as a different imperative loop for each would lead to unfulfilled data dependencies. The freedom in statement order supports automatic parallelization, but also allowed programmers choice in how to structure the program once machine considerations were removed.

We reduced scheduling loops to scheduling canonical attribute grammars. Our insight is that, for a restricted language of relative indices, we can schedule several unrolled loop steps and generalize the schedule to the rest. Section ?? discusses this in more detail.

Embedded Domain Specific Language: Functional Rendering

We designed our system for interaction with other tools and languages. A key ability is to invoke externally-defined functions, such as `max()` of Figure 2.9 for the maximum of two numbers and `paintRect()` of Figure 2.8 to draw a rectangle to the screen. Attribute grammars are compiled to run in some host system, such as JavaScript or OpenCL, and any function in scope to the generated code may be called.

Functions can be safely embedded as long as they provide a *pure* interface. In particular, the returned output should only depend on the inputs. Likewise, functions should be reentrant for use in automatic parallelization. In the case of embedding in statically checked languages, the host’s static checker is responsible for checking usage.

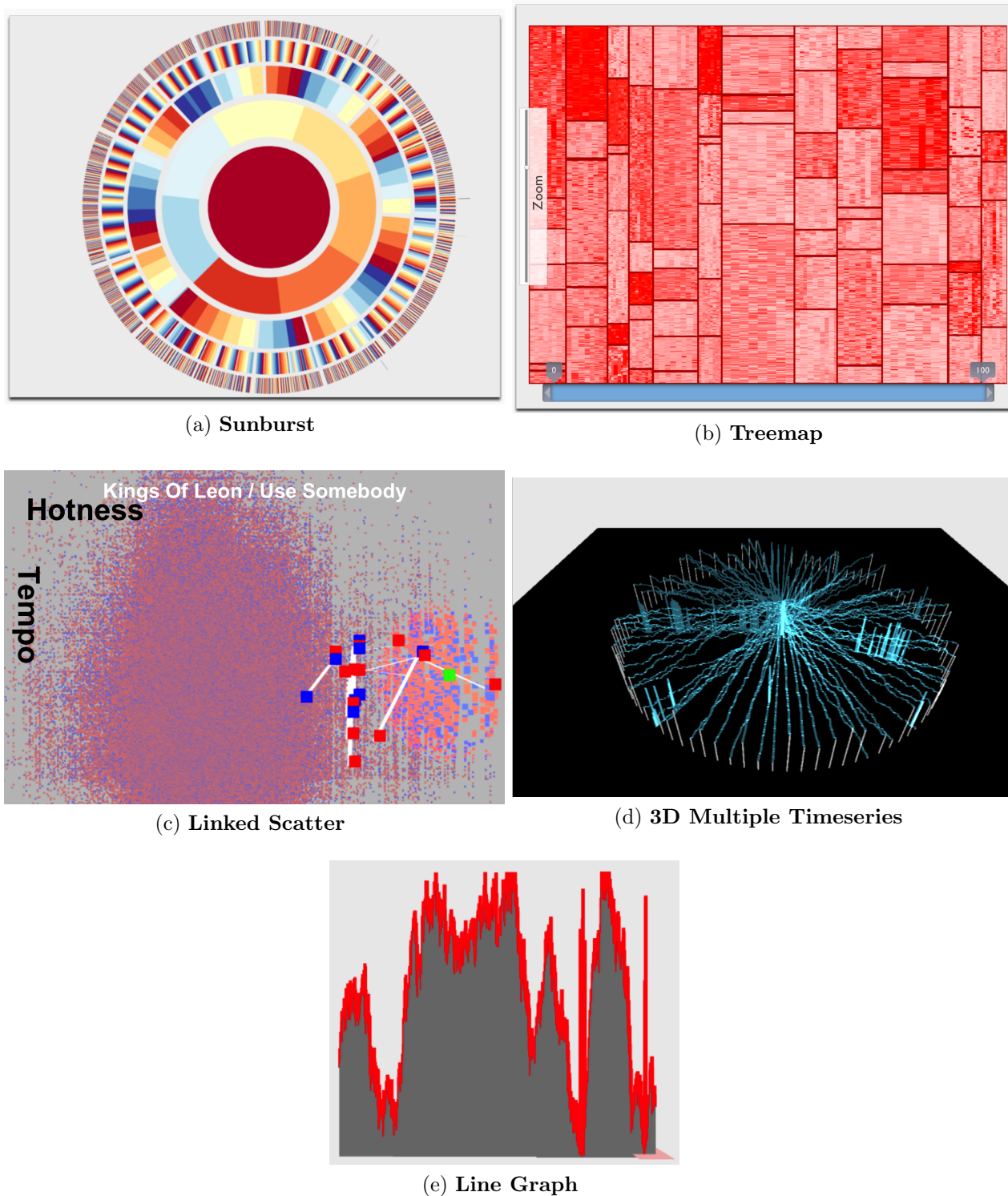
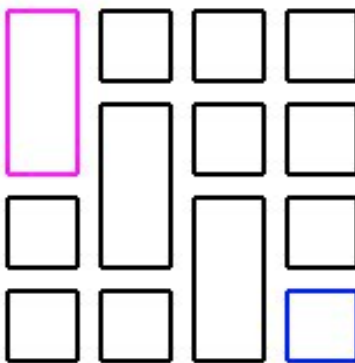


Figure 2.10: **Visualization screenshots.** All except [[CITE]] are interactive or animated. Each one was declaratively specified with our extended form of attribute grammars and automatically parallelized. Labels describe whether GPU or multicore code generation was used.



(a) HTML Tables (grid-based)

Main Page

From Wikipedia, the free encyclopedia

Jump to: [navigation](#), [search](#)

Welcome to Wikipedia ,

the free encyclopedia that anyone can edit .

3,800,580 articles in English

Today's featured article

Banksia cuneata is an endangered species of flowering plant in the Proteaceae family. Endemic to southwest Western Australia, it belongs to the genus Banksia which contains over 150 species, most with flower clusters that are cone-shaped, rather than the characteristic Banksia flower spike. A shrub or small tree up to 5 m tall, it has prickly foliage and pink and cream flowers. The common name Matchstick Banksia arises from the bloom in late bud, the individual buds of which resemble matchsticks. The species is pollinated by honeyeaters. Although B. cuneata was first collected before 1860, it was not until 1981 that Australian botanist Alex George formally described and named the species. Threatened by habitat loss and population growth, no longer found in the wild, the species is classified as endangered, surviving in fragments of remnant bushland in a region which has been 92% cleared for agriculture. As Banksia cuneata is killed by fire and regenerates from seed, it is highly sensitive to bushfire frequency. Fewer recurring within four years could wipe out populations of plants not yet mature enough to set seed. Banksia cuneata is rarely cultivated, and its prickly foliage limits its suitability to the cut flower industry. (more...)

Recently featured: [Battle of Barossa](#) • [Rutherford B. Hayes](#) • [Kevin O'Halloran](#)

Archive - By email - More featured articles...

Did you know...

From Wikipedia's newest content :

... that Kugelbake is the name of a series of tall wooden structures (current structure pictured) built at the mouth of the River Elbe for more than 300 years to aid mariners?
... that logical positivist A.J. Ayer believed that religious language was meaningless because it could not be verified empirically?
... that the *Body of Proof* episode "Dead Man Walking" guest starred Christina Hendricks as a potential love interest for main character Dr. Jennifer Quinn?
... that the Italian island of Montecristo , although 10.39 km² (4.01 sq mi) in area, is almost deserted, having only two inhabited inhabitants?
... that the 19th-century American female seminary movement, which aimed to give women educational opportunities, lent its name to a pair of similarly named institutions in Charleston, South Carolina , and Chelteown, Massachusetts ?
... that Malcolm X was nominated for an Academy Award in 1973? Archive - Start a new article - Nominate an article

Today's featured picture

The Alamo is a Roman Catholic mission located in San Antonio, Texas , United States. It was the site of the [Battle of the Alamo](#) during the [Texas Revolution](#) , in which almost all the Texian Army defenders were killed. Today, it is one of the most popular historic sites in the US.

Photo: Daniel Schwen

Recently featured: [Tungsten](#) - [Chicago skyline](#) - [Mount Rushmore](#)

Archive - More featured pictures...

• Arts

• Biography

• Geography

• History

• Mathematics

• Science

• Society

• Technology

• All portals

In the news

• [Vladimir Putin \(pictured\) is elected President of Russia](#) for a third term.
• [A series of explosions at an arms dump in Brazzaville](#), Republic of the Congo, kill at least 236 people and injure hundreds more.
• [A train crash near Szczekociny](#), Poland, kills 16 people.
• [A tornado outbreak in the Midwest and Southeastern United States](#) causes at least 39 fatalities.
• [BHP agrees to pay US\\$7.8 billion to plaintiffs affected by the Deepwater Horizon oil spill](#) .
• [English musician Davy Jones](#), a member of the rock band The Monkees, dies at the age of 66. Conflict in Syria
continues - Recent deaths - More current events...

• [1447 - Tommaso Parentucelli became Pope Nicholas V](#) .
• [1834 - York, Upper Canada , was incorporated as Toronto](#) .
• [1853 - Giuseppe Verdi 's *La traviata* premiered at Venice 's La Fenice](#) , but the performance was so bad that it caused the Italian composer to revise portions of the opera.
• [1899 - German chemical and pharmaceutical company Bayer registered Aspirin as a trademark](#) .
• [1945 - Petru Groza \(pictured\) of the Ploughmen's Front became the first Prime Minister of the Communist-dominated coalition government of Romania](#) .
• [1952 - In a last-minute decision, Nasir of Nigeria and his son Muhammad announced that American boxer Cassius Clay would change his name to Muhammad Ali](#) .
• [1988 - In Operation Flavus , the British Special Air Service killed three Provisional Irish Republican Army volunteers conspiring to bomb a parade of British military bands in Gibraltar](#) .
More anniversaries: March 5 - March 6 - March 7

Archive - By email - List of historical anniversaries

It is now March 6, 2012 (UTC) - Refresh this page

(b) CSS (flow-based)

Figure 2.11: Document layout screenshots.

2.4 Evaluation: Mechanized Layout Features

We specified many common layout language features with our extended form of attribute grammars. Most examples were written with few, if any, modifications to the generated code. This experience shows that our restricted form of attribute grammars are a viable formalism for layout specification. The following subsections present highlights from our case studies in specifying layouts with attribute grammars, and the appendix contains the full code.

Rendering

We found several rendering patterns to be important for many visualizations. A library of functional graphics primitives, such as `paintRect` in Figure 2.8, sufficiently augmented our attribute grammar language in order to achieve them.

- **2D and 3D.** Our base primitives are 3D, and we provide 2D primitives that reduce into them.
- **Color.** Our functional graphics primitives take an RGBA value as input, which enables controlling hue, luminosity, and opacity.
- **Linked view.** Multiple renderable objects can be associated with one node, which we can use for providing different views of the same data. Such functionality is common for statistical analysis software:

```
render := Circle(x,y,r) + Circle(offsetX + abs(x), offsetY + abs(y), r);
```

- **Zooming.** We can use the same multiple representation capability for a live zoomed out view (“picture-in-picture”):

```
render :=
  Circle(x, y, radius)
  + Circle(xFrame + x*zoom, yFrame + y*zoom, radius *zoom);
```

- **Visibility toggles.** Our macros support conditional expressions, which enables controlling whether to render an object. For example, a boolean input attribute can control whether to show a circle: `render := isOn ? Circle(0,0,10) : 0;`
- **Alternative representations.** Conditional expressions also enable choosing between multiple representations, not just on/off visibility:

```
render :=
  isOff ? 0
  : mouseHover ? CircleOutline(0,0,10)
  : Circle(0,0,10,5) ;
```

Non-Euclidean: Sunburst Diagram

Visualizations often require non-Euclidean layouts, such as the polar layout for the Sunburst diagram. Instead of propagating and computing over Euclidean values such as x and y coordinates as in H-AG, the visualization can use some other.

For example, in a sunburst diagram, a node should be rendered far from the center of the chart if it's level is high. In our implementation, each node transitively computes its radius as a function of its parent's. Likewise, the center of visualization propagates from parent to child, with the root node representing the center:

```
class Radial : Node {
    ...
    loop child {
        child.parentTotR := parentTotR + r;
        child.rootCenterX := rootCenterX;
        child.rootCenterY := rootCenterY;
    }
    ... Arc(rootCenterX, rootCenterY, show * (parentTotR + r), ...);
}
```

The full example is available in Appendix ??.

Charts: Line graphs

Animation and Interaction: Treemap

Flow-based: CSS Box Model

Grid-based: HTML Tables

2.5 Related Work

- loose formalisms: browser impl (C++), d3 (JavaScript), latex formulas (ML)
- restricted formalisms: cassowary and hp, UREs
- AGs: html tables

Chapter 3

A Safe Scheduling Language for Structured Parallel Traversals

3.1 Motivation and Approach

- structure is good for parallelization
- parallelization needs checking
- structured parallelism in layout

3.2 Background: Static Sequential and Task Parallel Visitors

Sequential Visitors

- Knuth: synth and inh
- OAG

Task Parallel Visitors

- FNC-2 / Work stealing

3.3 Structured Parallelism in Visitors

td, bu, in order

(related to distributed?)

concurrent

(old paper: unstructured within visit)

multipass

(any old paper? unstructured within visit)

nested

3.4 A Behavioral Specification Language

Formalism

3.5 Schedule Compilation

Phrase as rewrites working in an EDSL w/ templates

Rewrite rules

3.6 Schedule Verification

Overview

- properties to prove: schedule followed (and complete), dependencies realizable
- structure of proof

Axioms

- axioms
- examples from each

Proof

3.7 Automatically Staging Memory Allocation for SIMD Rendering

```
float *drawCircle (float x, float y, float radius) {
    float *buffer = malloc( (2 * sizeof(float) ) * round(radius))
    for (int i = 0; i < round(radius); i++) {
        buffer[2 * i] = x + cos(i * PI/radius);
        buffer[2 * i + i] = y + sin(i * PI/radius );
    }
    return buffer;
}
```

(a) **Naive drawing primitive .**

```
int allocCircle (float x, float y, float radius) {
    return round(radius);
}
```

(b) **Allocation phase of drawing.**

```
int fillCircle(float x, float y, float radius, float *buffer) {
    for (int i = 0; i < round(radius); i++) {
        buffer[2 * i] = x + cos(i * PI/radius);
        buffer[2 * i + i] = y + sin(i * PI/radius );
    }
    return 0;
}
```

(c) **Tessellation phase of drawing.**

Figure 3.1: Partitioning of a library function that uses dynamic memory allocation into parallelizable stages.

Problem

Dynamic memory allocation provides significant flexibility for a language, but it is unclear how to perform it on a GPU without significant performance penalties. This needed ended up leading to both performance and programmability issues in our design of a tessellation library that connects our GPU layout engine to our GPU rendering engine. Our insight is that the memory allocation may be staged using a variant of prefix sum node labeling. One pass gathers memory requests, a bulk allocation for the total amount is made, and then a scatter pass provides each node with a contiguous memory segment of it. We found manipulating memory addresses in this way to be error-prone, so we show how to use our synthesizer to automatically schedule use of the parallel memory allocator. Furthermore, we show how to syntactically hide the use of our allocation scheme through a macro that automatically expands into staged dynamic memory allocation and consumption calls.

For example, we found parallel dynamic memory allocation to simplify the transition between layout and rendering. All nodes that render a circle will call some form of drawCircle in Figure 3.1a. Depending on the size of the circle, which is computed as part of the layout traversals, a different amount of memory will be allocated. Once the memory is allocated, vertices will be filled in with the correct position. The rendering engine will then connect the vertices with lines and paint them to the screen. The processing of converting the abstract shape into renderable vertices is known as tessellation. We want our system to tessellate the

```
CBOX → BOX1 BOX2
{
    ...
    CBOX.render =
        drawCircle(CBOX.x, CBOX.y, CBOX.radius)
        + drawCircle(CBOX.x + 10, CBOX.y + 10, CBOX.radius * 0.5);
}

(a) Call into inefficient library.

CBOX → BOX1 BOX2
{
    ...
    CBOX.sizeSelf =
        allocCircle(CBOX.x, CBOX.y, CBOX.radius)
        + allocCircle(CBOX.x + 10, CBOX.y + 10, CBOX.radius * 0.5);
    CBOX.size = CBOX.sizeSelf + BOX1.size + BOX2.size;
    BOX1.buffer = CBOX.buffer + CBOX.sizeSelf;
    BOX2.buffer = BOX1.buffer + BOX1.size;
    CBOX.render =
        fillCircle(CBOX.x, CBOX.y, CBOX.radius, CBOX.buffer)
        + fillCircle(CBOX.x + 10, CBOX.y + 10, CBOX.radius * 0.5,
                     CBOX.buffer + allocCircle(CBOX.x, CBOX.y, CBOX.radius));
}

(b) Macro-expanded calls into staged library.

CBOX → BOX1 BOX2
{
    ...
    CBOX.render =
        @Circle(CBOX.x, CBOX.y, CBOX.radius)
        + @Circle(CBOX.x + 10, CBOX.y + 10, CBOX.radius * 0.5);
}

(c) Sugared calls into staged library.
```

Figure 3.2: Use of dynamic memory allocation in a grammar for rendering two circles.

display objects for each node in parallel.

Staged Parallel Memory Allocation

We stage the use of dynamic memory into four logical phases:

1. Parallel request (bottom-up tree traversal to gather)
2. Physical memory allocation
3. Parallel response (top-down tree traversal to scatter)
4. Computations that consume dynamic memory (normal parallel tree traversals)

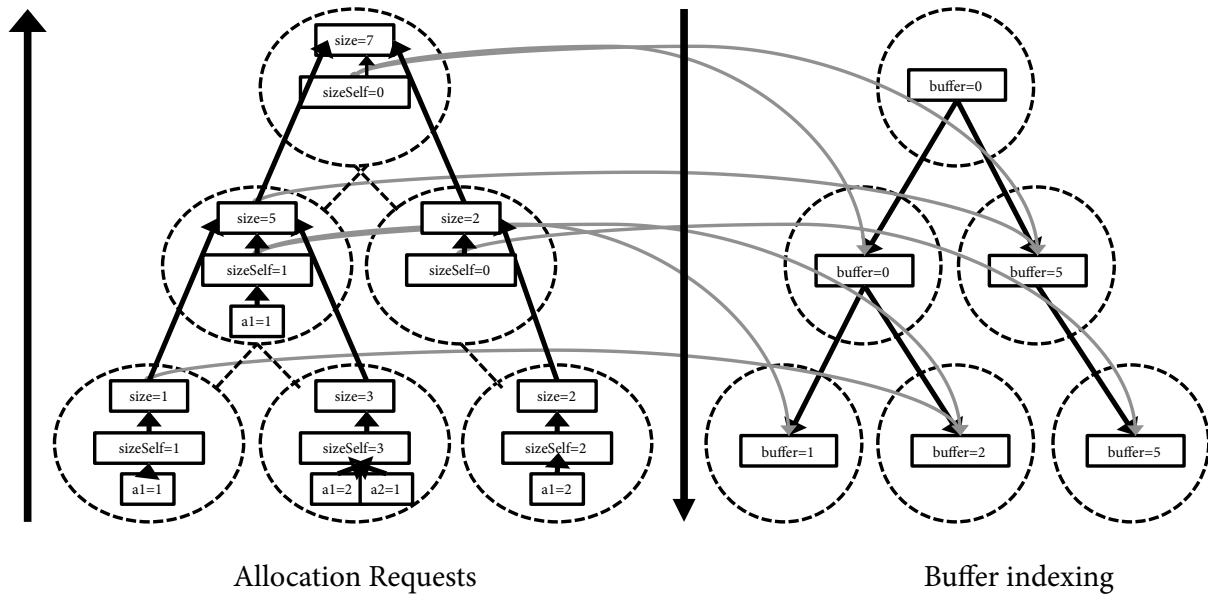


Figure 3.3: Staged parallel memory allocation as two tree traversals. First pass is parallel bottom-up traversal computing the sum of allocation requests and the second pass is a parallel top-down traversal computing buffer indices. Lines with arrows indicate dynamic data dependencies.

The staging allows us to parallelize the request and response stages. We reuse the parallel tree traversals for them, as well as for the actual consumption. The actual allocation of physical memory in stage 2 is fast because it is a single call. Figure 3.3 shows the dynamic data dependencies and two parallel tree traversals for an instance of staged parallel memory allocation.

Library functions that require dynamic memory allocation are manually rewritten into allocation request (Figure 3.1b) and memory consumption fragments (Figure ??). The transformation was not onerous to perform on our library primitives and, in the future, might be automated.

Invocations of the original in the attribute grammar are rewritten to use the new primitives. For example, drawing two circles (Figure 3.2a) is split into calls for allocation requests, buffer pointer manipulation, and buffer usage (Figure 3.2b). The transformation increases memory consumption costs due to book keeping of allocation sizes.

The result of our staging is three logical parallel passes, which, in practice, is merged into two parallel passes over the tree. The first pass is bottom up, similar to a prefix sum: each node computes its allocation requirements, adds that to the allocation requirements of its children, and then the process repeats for the next level of the tree. The *sizeSelf* and *size* attributes are used for the first pass. Once the cumulative memory needs is computed,

a bulk memory allocation occurs, and then a parallel top-down traversal assigns each node a memory span from `buffer` to `buffer + selfSize`. Finally, the memory can be used for actual computations through normal parallel passes. Memory use can occur immediately upon computation of the buffer index, so the last two logical stages are merged in implementation.

Automation with Automatic Scheduling and Macros

Manually manipulating the allocation requests and buffer pointers is error prone. We eliminated the problem through two automation techniques: automatic scheduling to enforce correct parallelization and macro expansion to encapsulate buffer manipulation.

To enforce proper parallelization, we relied upon our synthesizer to schedule the calls. If the synthesizer cannot schedule allocation calls and buffer propagation, it reports an error. Our insight is that, implicit to our staged representation, we could faithfully abstract the memory manipulations as foreign function calls. Our synthesizer simply performs its usual scheduling procedure.

To encapsulate buffer manipulation, we introduced the macro '`@`'. Code that uses it is similar to code that assumes dynamic memory allocation primitives: the slight syntactic difference can be seen between Figure 3.2c and Figure 3.2a. Our macros (implemented in OMetaJS [[CITE]]) automatically expand into the form seen in Figure 3.2b.

Our use case only required one allocation stage, but multiple may be needed. For example, a final logging stage might be added that should run after all other computations, including rendering. However, the '`@`' calls described above expand to contribute to one attribute (`size`): no allocation is made until all of the sizes are known, which prevents making an allocation after using dynamic memory. To support multiple allocation stages, the '`@`' macro could be expanded to include logical group names: `@[render]Circle (...)` would contribute to `sizeRender`, `@[log]error (...)` to `sizeLog`, and `@[render,log]Strange (...)` to both `sizeRender` and `sizeLog`. Parallel traversals would be created for each logical name, and the synthesizer would be responsible for determining if the traversals can be merged in the final schedule and implementation.

3.8 Scheduling Loops

3.9 Evaluation: Layout as Structured Parallel Visits

Box model

Nested text

Grids

SIMD Rendering through Staged Memory Allocation

We evaluate three dimensions of our staged memory allocation approach: flexibility, productivity, and performance. First, it needs to be able to express the rendering tasks that we encounter in GPU data visualization. Second, it should some form of productivity benefit for these tasks. Finally, the performance on those tasks must be fast enough to support real-time animations and interactions of big data sets.

Productivity

Productivity is difficult to measure. Before using the automation extensions for rendering, we repeatedly encountered bugs in manipulating the allocation calls and memory buffers. The bugs related both to incorrect scheduling and to incorrect pointer arithmetic. Our new design eliminates the possibility of both bugs.

One suggestive productivity measure is of how many lines of code the macro abstraction eliminates from our visualizations. We measured the impact on using it for 3 of our visualizations. The first visualization is our HBox language extended with rendering calls, while the other two are interactive reimplementations of popular visualizations: a treemap [[CITE]] and multiple 3D line graphs [[CITE]].

Table 3.1: Lines of Code Before/After Invoking the '@' Macro

Visualization	Before (loc)	After (loc)	Decrease
HBox	97	54	44%
Treemap	296	241	19%
GE	337	269	20%

Table 3.1 compares the lines of code in visualizations before and after we added the macros. Using the macros eliminated 19–44% of the code. Note that we are *not* measuring the macro-expanded code, but code that a human wrote.

As shown in Figure 3.2, the eliminated code is code that was introduced by staging the library calls. Porting unstaged functional graphics calls to the library, is in practice, an alpha

renaming of function names. Using the '@' macro eliminates 19–44% of the code that would have otherwise been introduced and completely eliminates two classes of bugs (scheduling and pointer arithmetic), so the productivity benefit is non-trivial.

Performance

3.10 Related Work

Lang of schedules

- background
- stencils and skeletons: wavefront, ...
- polyhedra

Schedule verification

- compare to OAG etc., looser dataflow/functional langs

Chapter 4

Interacting with Automatic Parallelizers through Schedule Sketching

4.1 Automatic Parallelization: The Good, the Bad, and the Ugly

The Good: Automating Dependency Management

The Bad: Guiding Parallelization

The Ugly: Preventing Serialization

4.2 Holes

4.3 Generalizing Holes to Unification

4.4 Case Studies: Sketching in Action

Show use in CSS and data viz:

- when automatic is fine
- when sketch needed for checking/debugging
- when sketch needed for sharing

4.5 Related Work

- sketch, sketch for concurrent structures
- oopsla paper for individual traversals

Chapter 5

Parallel Schedule Synthesis

5.1 Motivation: Fast and Parameterized Algorithm Design

5.2 Optimized Algorithm: Finding One Schedule

5.3 Optimized Algorithm: Autotuning Over Many Schedules

Alternation Heuristic: Off-by-one Optimality

Enumeration via Incrementalization

5.4 Complexity Analysis and the Power of Sketching

5.5 Evaluation

Speed of synthesis

Success, fail, enumerate

Line counts of extensions

Loss from greedy heuristic

Benefit from autotuning

Chapter 6

Optimizing Tree Traversals for MIMD and SIMD

6.1 Overview

For a full language, statically identified parallelization opportunities still require an efficient runtime implementation that exploits them. In this section, we show how to exploit the logical concurrency identified within a tree traversal to optimize for the architectural properties of two types of hardware platforms: MIMD (e.g., multicore) and SIMD (e.g., sub-word SIMD and GPU) hardware. For both types of platforms, we optimize the schedule within a traversal and the data representation. We innovate upon known techniques in two ways:

- 1. Semi-static work stealing for MIMD:** MIMD traversals should be optimized for low overheads, load balancing, and locality. Existing techniques such as work stealing provide spatial locality and, with tiling, low overheads. However, dynamic load balancing within a traversal leads to poor temporal locality across traversals. The processor a node is assigned to in one traversal may not be the same one in a subsequent traversal, and as the number of processors increases, the probability of assigning to a different one increases. Our solution dynamically load balances one traversal and, due to similarities across traversals, successfully reuses it.
- 2. Clustering traversals for SIMD:** SIMD evaluation is sensitive to divergence across parallel tasks in instruction selection. Visits to different types of tree nodes yield different instruction streams, so naive vectorization fails for webpages due to their visual variety. Our insight is that similar nodes can be semi-statically identified. Thus *clustered* nodes will be grouped in the data representation and run in SIMD at runtime.

Our techniques are important and general. They overcame bottlenecks preventing seeing any speedup from parallel evaluation for webpage layout and data visualization. Notably, they are generic to computations over trees, not just layout. An important question going forward is how to combine them as, in principle, they are complementary.

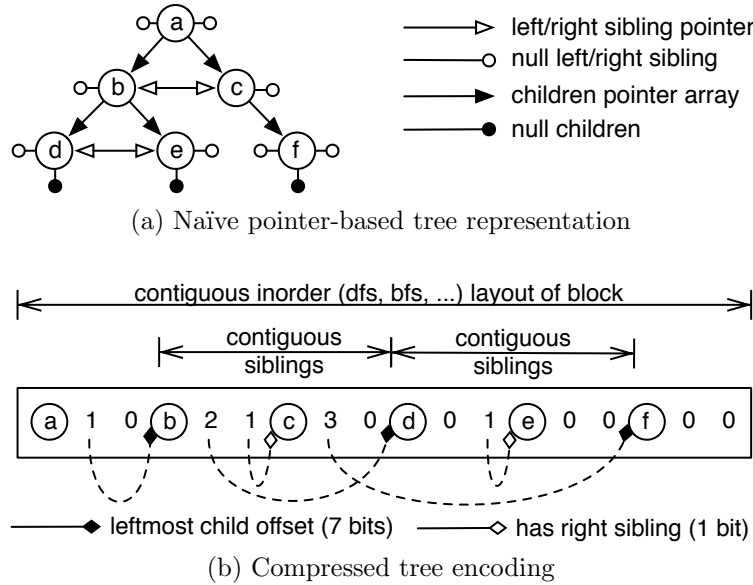


Figure 6.1: Two representations of the same tree: naïve pointer-based and optimized. The optimized version employs packing, breadth-first layout, and pointer compression via relative indexing.

6.2 MIMD: Semi-static work stealing

We optimize the tree data representation and runtime schedule for MIMD evaluation. We did not see significant parallel speedups when either one was left out. Through a non-trivial amount of experimentation, we found an almost satisfactory combination of existing techniques. It includes popular ideas such as work stealing [[CITE]] for load-balanced runtime scheduling and tiling [[CITE]] for data locality, so we report on how to combine them. However, we did not see more than 2X speedups until we added a novel technique to optimize for low run-time scheduling overheads and temporal data locality: semi-static work stealing. The remainder of this section explores our basic data representation and runtime scheduling techniques.

Data representation: Tuned and Compressed Tiles

Our data representation optimizes for spatial and temporal locality and, as will be used by the scheduler, low overheads for operating over multiple nodes. Many researchers have proposed individual techniques for similar needs, and it is unclear which to use for what hardware. For example, mobile devices typically have smaller caches than laptops, they should exchange time for space. Our solution was to implement many techniques and build an autotuner [[CITE]] that automatically choose an effective combination.

Our autotuner runs sample data on multiple configurations for a particular platform to

decide which configuration to use. The most prominent options are:

- C++ collections or contiguous arrays
- tiling [**tiling**] of subtrees
- depth-first or breadth-first ordering of nodes in a tile (with matching traversal order [**Chilimbi:1999**])
- aligned data, or unaligned but more packed data
- pointer compression

Several of the techniques are parameterized, so our tuner performs a brute force search for parameter values such as the maximum size of a subtree tile. To make the search tractable, we prune by manually providing heuristics, such as for parameter ranges.

The individual optimizations target several objectives:

- **Compression** Compressing the tree better utilizes memory bandwidth and decreases the working set size. We use two basic techniques: structure packing and pointer compression. Packing combines several fields in the same word of memory, such as storing 32 boolean attributes in one 32bit integer field. Similar to **compression** [**compression**], compression encodes node references as relative offsets (16–20bits) rather than 32bit of 64bit pointers. Likewise, as there are typically few siblings, instead of a counter of number of children (or siblings), we use an `isLastSibling` bit. Figure 6.1 depicts a tree using pointers and one of our representations: in the example, the compressed form uses 96% fewer bits on a 64-bit architecture.
- **Temporal and Spatial Locality** The above compression optimizations improve locality by decreasing the distance between data. To further improve locality, we support rearranging the data in several ways .

Tiling [**tiling**] cuts the tree into subtrees and collocates nodes of the same subtree. It improves spatial locality because a node only reads and writes to its neighbors. Likewise, we support breadth-first and depth-first node orderings within a subtree (and across subtrees). Such a representation matches the tree traversal order [**Chilimbi:1999**] and therefore improves temporal locality.

- **Prefetching** We supports several options for prefetching to avoid waiting on data reads. First, the data access patterns with the data layout, so hardware prefetchers might automatically predict and prefetch data. Second, our compiler can automatically insert explicit prefetch instructions as part of the traversal. Finally, runahead processing [**runaheadprocessing**] pre-executes data access instructions. A helper thread traverses a subtree ahead of a corresponding evaluator thread, requesting node data while the evaluator is still computing an earlier thread. We only saw benefits of the first in practice, but leave the others as tunable.

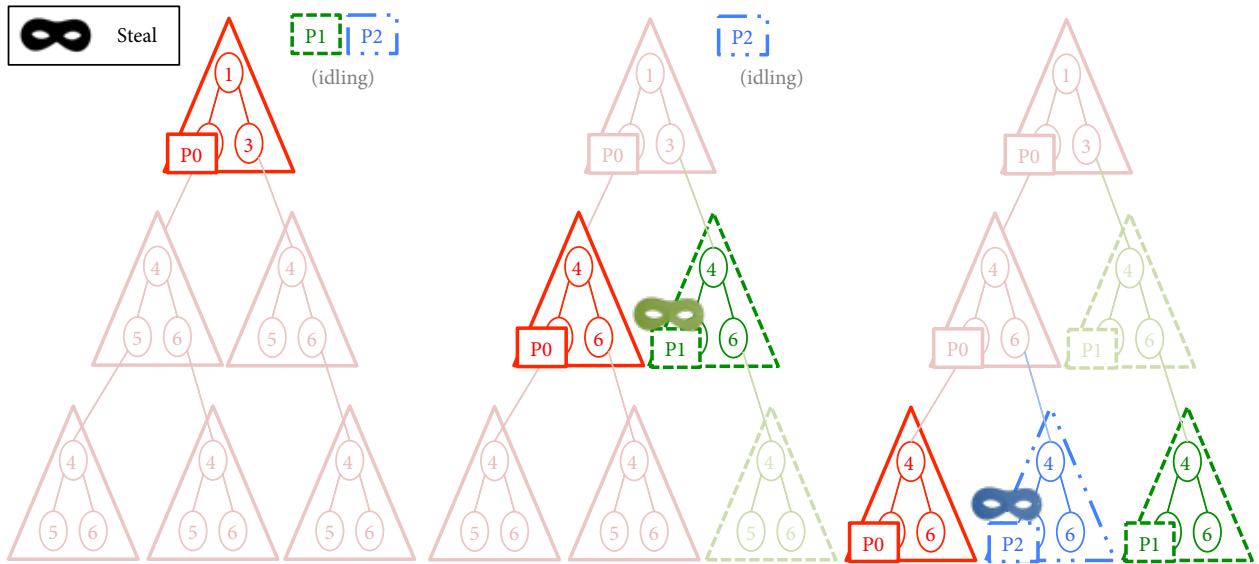


Figure 6.2: **Simulation of work stealing.** Top-down simulated tree traversal of a tiled tree by three processors in three steps.

- **Parallel scheduling.** Reasoning about individual nodes, such as for load balancing and synchronization, leads to high overheads. By scheduling tiles rather than nodes, we cut overheads. Nodes correspond to tasks in our system, so our approach is a form of *coarsening*. Furthermore, different synchronization strategies are possible for tiles, such as whether to use spin locks, so we autotune over the implementation options.

We also support several scheduling options. First, we support third-party task schedulers, including Intel TBB [[CITE]], Cilk [[CITE]], and those of TesselationOS [[CITE]]. Second, we built our own that uses a variant of work-stealing threads pinned to processors. It includes options such as whether to use hyper threads or not, and as we saw low speedups when using multiple sockets, how many threads to use. Our autotuner picks between scheduler implementations.

Figure 6.1 depicts several of the data representation optimizations: packing, pointer compression, and a breadth-first layout.

Scheduling: Semi-static Work Stealing

We optimize our tree traversal task scheduler for low overheads, high temporal and spatial data locality, and load balancing. Webpages are relatively small and use many traversals, so we found that aggressively optimizing individual traversals to be an important implementation concern. Our approach is to combine static scheduling [[CITE]] with dynamic work stealing. We semi-statically schedule a traversal over the tree to as soon as it is available and

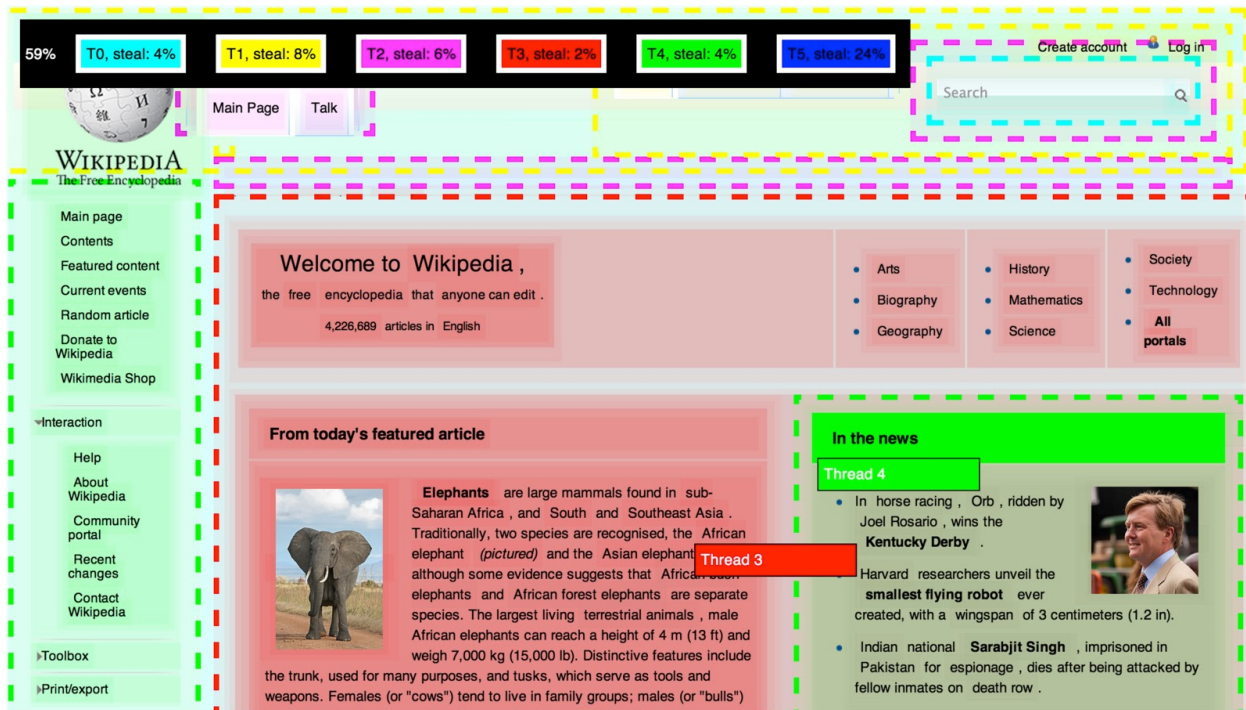


Figure 6.3: **Simulation of work stealing on Wikipedia.** Colors depict claiming processor and dotted boundaries indicate subtree steals. Top-left boxes measure hit rate for individual processor.

reuse that schedule across traversals: this optimizes for temporal locality and low over-heads. We use work stealing as a heuristic for computing the first tree traversal for approximate load balancing. We did not see significant speedups with the base approaches on their own, but our combination led to 7X parallel speedups.

Our algorithm schedules the first traversal using work stealing [[CITE]]. Work stealing was introduced as a dynamic scheduling algorithm that provides load balancing and spatial locality. Figure 6.2 depicts a trace of three processors performing work stealing. Each processor operates on an internal task queue, and whenever a processor exhausts its internal queue, it will *steal* from another processor's queue. In the case of a top-down tree traversal, acting upon an internal queue corresponds to a depth-first traversal of a subtree, and stealing corresponds to transferring ownership of an untraversed subtree. We lower overheads on the first traversal in two ways: we perform task coarsening by scheduling tiles rather than individual nodes, and we simulate the work stealing in one thread on a localized copy of the tiling meta data. The colors of Figure 6.3 show how different processors claim different nodes of a webpage during a parallel traversal: the localization of colors demonstrates the spatial locality of work stealing. Likewise, figure demonstrates that there are relatively few scheduling overheads (steals are indicated by dotted borders).

Work stealing suffers from runtime overheads and lack of temporal locality. To estimate



Figure 6.4: **Temporal cache misses for simulated work stealing over multiple traversals.** Simulation of 4 threads on Wikipedia. Blue shade represents a hit and red a miss. 67% of the nodes were misses. Top-left boxes measure hit rate for individual processor.

the overhead, we simulated work stealing for 6 processors on Wikipedia. Assuming uniform compute time per node, 5% of the nodes would trigger stealing. This cost is in addition to constant overhead to processing the internal per-processor task queues. The issue with temporal locality is that a node will be assigned to different processors across multiple traversals. Figure 6.4 shows which nodes must move across processors in a simulation 4 processors performing a sequence of two traversals. 67% of the nodes are red, indicating substantial movement. Both the steal rate and temporal miss rate worsen as the number of processors increase.

We use work stealing as a heuristic for semi-static scheduling so that the strengths of one address the weaknesses of the other. Semi-static scheduling precomputes the traversal order for each processor, which eliminates runtime overheads. Computing a load-balanced schedule can be quite expensive, however, because optimality is NP [[CITE]]. Instead, we use work stealing as a heuristic by running a simulation in which the cost of each tile is the

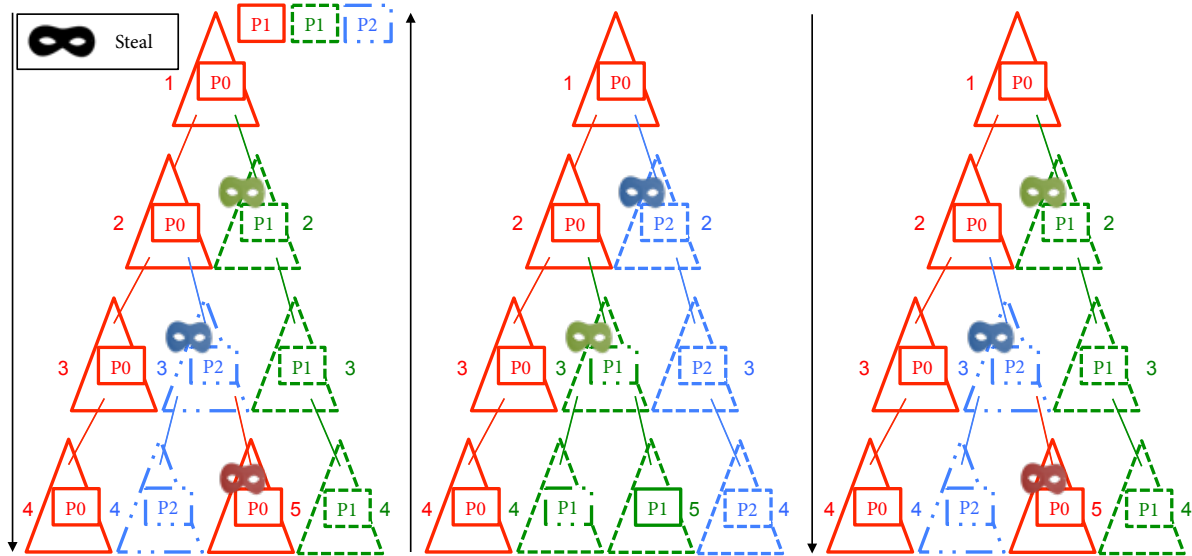


Figure 6.5: **Dynamic work stealing for three traversals.** Tiles are claimed by different processors in different traversals.

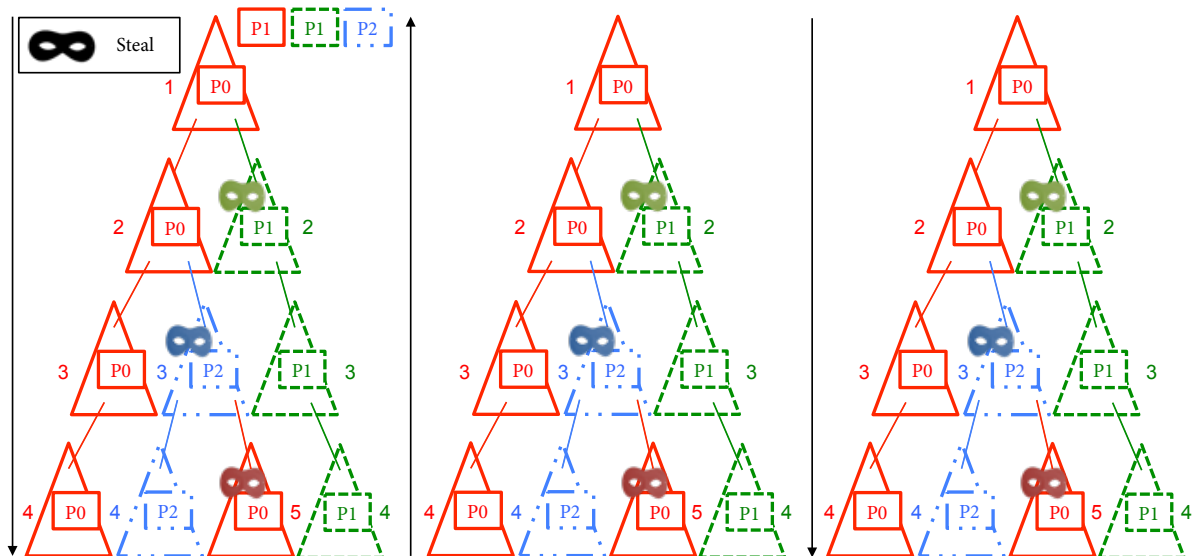


Figure 6.6: **Semi-static work stealing.** Dynamic schedule for first traversal is reused for subsequent ones.

number of nodes in it and penalizing simulated steals. The trace through the simulation for a top-down traversal is used as the schedule for top-down traversals, and the reverse for bottom-up. Computing the schedule is fast – a linear traversal over the tile meta data.

Our approach achieves low overheads, high temporal and spatial locality locality, and load balanced evaluation. Temporal locality is enforced by reusing the same schedule across the traversals, and semi-static scheduling with a fast heuristic provides low overheads. Our work stealing heuristic provides spatial locality and an approximate form of load balancing.

Evaluation

6.3 SIMD Background: Level-Synchronous Breadth-First Tree Traversal

The common baseline for our two SIMD optimizations is to implement parallel preorder and postorder tree traversals as level-synchronous breadth-first parallel tree traversals. Reps first suggested such an approach to parallel attribute grammar evaluation [[CITE]], but did not implement it. Performance bottlenecks led to us deviate from the core representation used by more recent data parallel languages such as NESL [[CITE]] and Data Parallel Haskell [[CITE]]. We discuss our two innovations in the next subsections, but first overview the baseline technique established by existing work.

The naive tree traversal schedule is to sequentially iterate one level of the tree at a time and traverse the nodes of a level in parallel. A parallel preorder traversal starts on the root node’s level and then proceeds downwards, while a postorder traversal starts on the tree fringe and moves upwards (Figure 6.7 6.7a). Our MIMD implementation, in contrast, allows one processor to compute on a different tree level than another active processor. In data visualizations, we empirically observed that most of the nodes on a level will dispatch to the same layout instructions, so our naive traversal schedule avoids instruction divergence.

The level-synchronous traversal pattern eliminates many divergent memory accesses by using a corresponding data representation. Adjacent nodes in the schedule are collocated in memory. Furthermore, individual node attributes are stored in *column* order through a array-of-structure to structure-of-array conversion. The conversion collocates individual attributes, such as the width attribute of one node being stored next to the width attribute of the node’s sibling (Figure 6.7c). The index of a node in a breadth-first traversal of the tree is used to perform a lookup in any of the attribute arrays. The benefit this encoding is that, during SIMD layout of several adjacent nodes, reads and writes are coalesced into bulk reads and writes. For example, if a layout pass adds a node’s padding to its width, several contiguous paddings and several contiguous widths will be read, and the sum will be stored with a contiguous write. Such optimizations are crucial because the penalty of non-coalesced access is high and, for layout, relatively few computations occur between the reads and writes.

Full implementation of the data representation poses several subtleties.

```

void parPre(void (*visit)(Prod &), List<List<Prod>> &levels) {
    for (List<Prod> level in levels)
        parallel_for (Prod p in level)
            visit(p)
}
void parPost(void (*visit)(Prod &), List<List<Prod>> &levels) {
    for (Array<Prod> level in levels.reverse())
        parallel_for (Prod p in level)
            visit(p)
}

```

(a) Level-synchronous Breadth-First Traversal

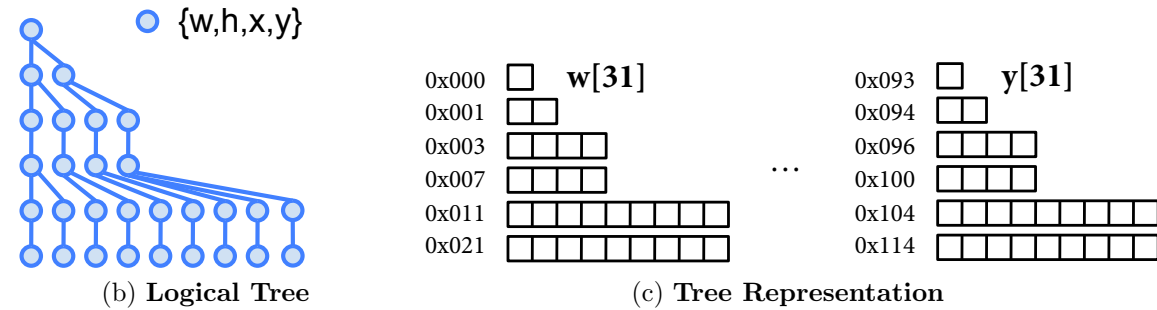


Figure 6.7: SIMD tree traversal as level-synchronous breadth-first iteration with corresponding structure-split data representation.

- **Level representation.** To eliminate traversal overhead, a summary provides the index of the first and last node on each level of a tree. Such a summary provides data range information for launching the parallel kernels that evaluate the nodes of a level as well as the information for how to proceed to the next level.
- **Edge representation.** A node may need multiple named lists of children, such as an HTML table with a header, footer, and an arbitrary number of rows. We encode the table's edges as 3 global arrays of offsets: header, footer, and first-row. To support iterating across rows, we also introduce a 4th array to encode whether a node is the last sibling. Thus, any named edge introduces a global array for the offset of the pointed-to node, and for iteration, a shared global array reporting whether a node at a particular index is the end of a list.
- **Memory compression.** Allocating an array the size of the tree for every type of node attribute wastes memory. We instead statically compute the maximum number of attributes required for any type of node, allocate an array for each one, and map the attributes of different types of nodes into different arrays. For example, in a language of HBox nodes as Circle nodes who have attributes 'r' and 'angle', 4 arrays will be allocated. The HBox requires an array for each of the attributes 'w', 'h', 'x', and 'y' while the Circle nodes only require two arrays. Each node has one type, and if that

type is HBox, the node’s entry in the first array will contain the ‘w’ attribute. If the node has type Circle, the node’s entry in the first entry will contain the ‘r’ attribute.

- **Tiling.** Local structural mutations to a tree such as adding or removing nodes should not force global modifications. As most SIMD hardware has limited vector lengths (e.g., 32 elements wide), we split our representation into blocks. Adding nodes may require allocation of a new block and reorganization of the old and new block. Likewise, after successive additions or deletions, the overall structure may need to be compacted. Such techniques are standard for file systems, garbage collectors, and databases.

In summary, our basic SIMD tree traversal schedule and data representation descend from the approach of NESL [[CITE]] and Data Parallel Haskell [[CITE]]. Previous work shows how to generically convert a tree of structures into a structure of arrays. Those approaches do not support statically unbounded nesting depth (i.e., tree depth), but our system supports arbitrary tree depth because our transformation is not as generic.

A key property of all of our systems, however, is that the structure of the tree is fixed prior to the traversals. In contrast, for example, parallel breadth-first traversals of graphs will dynamically find a minimum spanning tree [[CITE]]. Such dynamic alternatives incur unnecessary overheads when performing a sequence of traversals and sacrifice memory coalescing opportunities. Layout is often a repetitive process, whether due to multiple tree traversals for one invocation or an animation incurring multiple invocations, so costs in creating an optimized data representation and schedule are worth paying.

6.4 Input-dependent Clustering for SIMD Evaluation

Once the tree is available, we automatically optimize the schedule for traversing a tree level in a way that avoids instruction divergence. Our insight is that we can cluster tasks (nodes) based on node attributes that influence control flow. We match the data layout to the new schedule, and optimize the clustering process to prevent the planning overhead to outweigh its benefit. The overall optimization can be thought of an extension to loop unswitching where the predicate is input-dependent and a sorting prepass guarantees that subintervals will branch identically.

The Problem

The problem we address stems from layout being a computation where the instructions for each node are heavily input dependent. The intuition can be seen in contrasting the visual appearance of a webpage vs. a data visualization. Different parts of a webpage look quite different from one another, which suggests sensitivity to values in the input tree, while a visualization looks self-similar and thus does not use widely different instructions for different nodes. For an example of divergence, an HBox’s width is the sum of its children

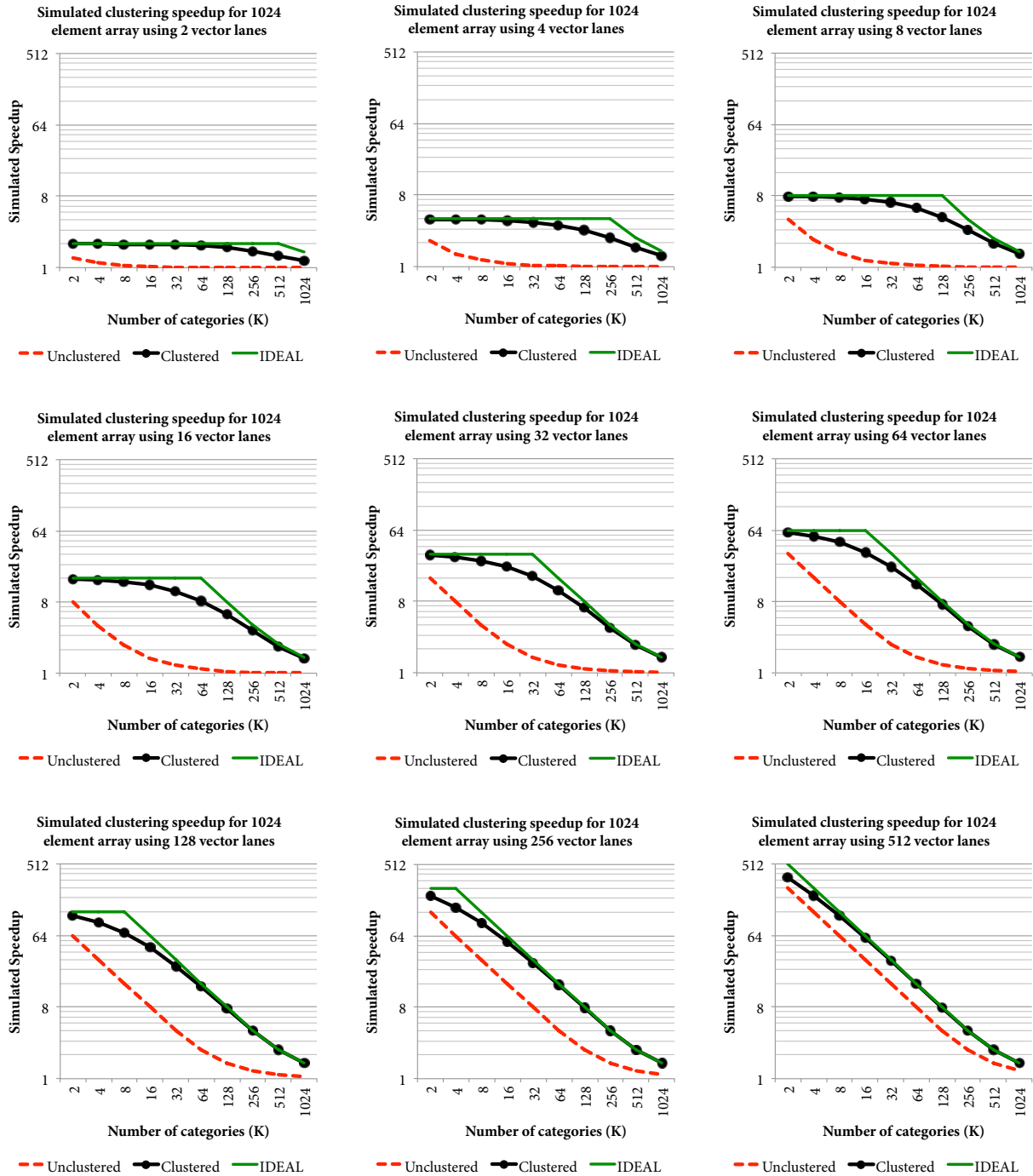


Figure 6.8: blah

```

void parPreClustered(void (*visit)(Prod &), List<List<Array<Prod>>> &levels) {
    for (List<Prod> level in levels)
        for (Array<Prod> cluster in level)
            parallel_for (Prod p in cluster)
                visit(p)
}

```

Figure 6.9: **ASDF**.

widths, while a VBox’s is their maximum. The visit to a node (Figure ??) will diverge in instruction selection based on the node type.

We ran a simulation to measure the performance cost of the divergence. Assuming a uniform distribution of types of nodes in a level, as the number of types of nodes go up (K), the probability that all of the nodes in a group share the same instructions drops exponentially. Figure 6.8 shows the simulated speedup for SIMD evaluation over a tree level of 1024 nodes on computer architectures with varying SIMD lengths. The x axis of each chart represents the number of types and the y axis is the speedup. As the number of choices increase, the benefit of the naive breadth-first schedule (red line) decreases. It is far from the ideal speedup, which we estimated as a function of the SIMD length of the architecture (maximal parallel speedup, contributing the horizontal portion of the green lines) and the expected number of different categories (mandatory divergences, contributing the diagonal portion).

Code Clustering

Our solution is to cluster nodes of a level based on the values of attributes that influence the flow of control. SIMD evaluation of the nodes in a cluster will be free of instruction divergence. Furthermore, by changing the data representation to match the clustered schedule, memory accesses will also be coalesced. We first focus on applying the clustering transformation to the code.

Figure 6.9 shows the clustered evaluation variant of the MIMD *parPre* traversal of Figure ???. The traversal schedule is different because the order is based on the clustering rather than breadth-first index. Changing the order is safe because the original loop was parallel with no dependencies between elements. Computing over clusters guarantees that all calls to a visit dispatch function in the parallel inner loop (e.g., of *visit1*) will branch to the same switch statement case. This modified schedule avoids instruction divergence.

Our loop transformation can be understood as a use of loop unswitching, which is a common transformation for improving parallelization. Loop unswitching lifts a conditional out of a loop by duplicating the loop inside of both cases of the conditional. Clustering establishes the invariant of being able to inspect the first item of a collection sufficing for performing unswitching for a loop over all of the items. Figure 6.10 separates our transformation of *visit1* (Figure ???) into using the same exemplar for the dispatch and then loop unswitching.

```

Prod firstProd = cluster[0]
parallel_for (prod in Cluster) {
    switch (firstProd.type) {
        case S → HBOX: break;
        case HBOX → ε:
            HBOX.w = input(); HBOX.h = input(); break;
        case HBOX → HBOX1 HBOX2:
            HBOX0.w = HBOX1.w + HBOX2.w;
            HBOX0.h = MAX(HBOX1.h, HBOX2.h);
            break;
    }
}

```

(a) Clustered dispatch.

```

Prod firstProd = cluster[0]
switch (firstProd.type) {
    case S → HBOX: break;
    case HBOX → ε:
        parallel_for (prod in Cluster) {
            HBOX.w = input(); HBOX.h = input();
        }
        break;
    case HBOX → HBOX1 HBOX2:
        parallel_for (prod in Cluster) {
            HBOX0.w = HBOX1.w + HBOX2.w;
            HBOX0.h = MAX(HBOX1.h, HBOX2.h);
        }
        break;
}

```

(b) Unswitched dispatch.

Figure 6.10: Loop transformations to exploit clustering for vectorization.

Clustering is with respect to input attributes that influence control flow, which may be more than the node type. For example, in our parallelization of the C3 layout engine, we found that the engine author combined the logic of multiple box types into one visit function because the variants shared a lot of code. He instead used multiple node flags to guide instruction selection. Both the node type and various other node attributes influenced control flow, and therefore our clustering condition was on whether they were all equal. Using all of the attributes led to too granular of a clustering condition, so we manually tuned the choice of attributes.

Data Clustering

The data representation should be modified to match the clustering order. The benefit is coalesced memory accesses, but overhead costs in performing the clustering should be considered.

Our algorithm matches the data representation order to the schedule by placing nodes of a cluster into the same contiguous array. Parallel reads and are coalesced, such as the inspection of the node type for the visit dispatch. Parallel writes are likewise coalesced.

Reordering data is expensive as all of the data is moved. In the case of our data visualization system, we can avoid the cost because the data is preprocessed on our server. For webpage layout, the client performs clustering, which we optimize enough such that the cost is outweighed by the subsequent performance improvements.

We optimize reordering with a simple parallel two-pass technique. The first pass traverses each level in parallel to compute the cluster for each node and tabulate the cluster sizes for each tree level. The second pass again traverses each level in parallel, and as each node is traversed, copies it into the next free slot of the appropriate cluster. Even finer-grained

parallelization is possible, but this algorithm was sufficient for lowering reordering costs enough to be amortized.

Nested Clustering

Clustering can also be used to address divergences induced by computations over neighboring nodes. They avoidable irregularities can take several forms:

- **Branches.** For the case of webpage layout, we saw cases where attributes of the parent node or children node influence instruction selection, such as whether to include a child node in a width computation. The properties can be included in the clustering condition to eliminate the corresponding instruction divergences.
- **Load imbalance in loops.** One node may have no children while another may have many. If the layout computation involves a loop, SIMD evaluation will perform the two loops in lock-step. Thus, as the nodes have different amounts of children, the SIMD lanes devoted to the first child will not be utilized: this is a load balancing problem. The number of children can be included in the clustering condition to eliminate load imbalance.
- **Random memory access in loops.** A further issue with lock-step loops over child nodes is memory divergence. A breadth-first layout would provide strided memory access, but if each level is clustered, the locations of a node’s children may be random without further aid. We found a *nested* solution where *subtrees* are assigned to clusters. Instead of just associating nodes of a level with a cluster, our algorithm then treats the nodes of a cluster as roots. It recursively expands a subtree such that all of the cluster nodes share it (with respect to the attributes influencing control flow). The data layout follows the nested clustering, so parallel memory accesses to the children of nodes will be coalesced.

Each of these clusterings introduce an invariant for a cluster for optimizing performance within that cluster. However, the clustering condition is more discriminating. Cluster sizes may decrease, which would significantly decrease performance if cluster size shrinks below vector length size. Our evaluation explores these options in practice.

6.5 Evaluation

MIMD Data Representation and Scheduling Optimizations

By statically exposing traversal structure (e.g., `parPre`) to our code generators, we observe sequential and parallel speedups. We separately evaluate the importance of the data representation optimizations from the scheduling ones on random 500-1000 node documents in the `hbox++` language. Finally, we examine the parallel benefit on webpages.

Configuration	Total speedup				Parallel speedup		
	Cores				Cores		
	1	2	4	8	2	4	8
TBB, server	1.2x	0.6x	0.6x	1.2x	0.5x	0.5x	1.0x
FTL, server	1.4x	2.4x	5.2x	9.3x	1.8x	3.8x	6.9x
FTL, laptop	1.4x	2.1x			1.6x		
FTL, mobile	1.3x	2.2x			1.7x		

Table 6.1: **Speedups and strong scaling across different backends (Back) and hardware.** Baseline is a sequential traversal with no data layout optimizations. FTL is our multicore tree traversal library. Left columns show total speedup (including data layout optimizations by our code generator) and right columns show just parallel speedup. Server = Opteron 2356, laptop = Intel Core i7, mobile = Atom 330.

Backend	Input	Parallel speedup		
		Cores		
		2	4	8
TBB	Wikipedia	1.5x	1.6x	1.2x
	xkcd Blog	1.5x	1.8x	1.2x
FTL	Wikipedia	1.6x	2.8x	3.2x
	xkcd Blog	1.5x	2.3x	3.1x

Table 6.2: **Parallel CSS layout engine.** Run on a 2356 Opteron.

We first evaluate the performance of our task scheduler (FTL in Table 6.1). Our comparison point is Intel’s TBB [`inteltbb`] dynamic task scheduler that performs work stealing [`cilk`], which was the most efficient third-party work stealing library that we tried. We included our data layout optimizations in all calculations because, without them, we saw no speedup. TBB causes slowdowns until achieving no cost (nor benefit) at 8 cores. Our insight is that it suffered from high overheads: switching to scheduling tiles by using our optimized data representation improved performance. Our semi-static working stealing scheduler, however, achieved a 6.9X speedup on 8 cores. We did not see significant further speedups for higher core counts, and hypothesize that it is due to the socket jump. We experimented with other schedulers, such as a simple for-loop over tiles near the fringe of the tree, but the achieved 2X speedup is much lower than the 6.9X of our semi-static work stealer.

Data representation was key to achieving parallel speedups. It achieved 1.2X-1.4X speedups for sequential processing (Table 6.1). However, on 4 cores, it improved performance from 2.8X without data representation optimizations to 5.2X when using them. The difference is 1.9X: our data representation optimizations both complement and improve scheduling optimizations. Without them, parallel performance was poor.

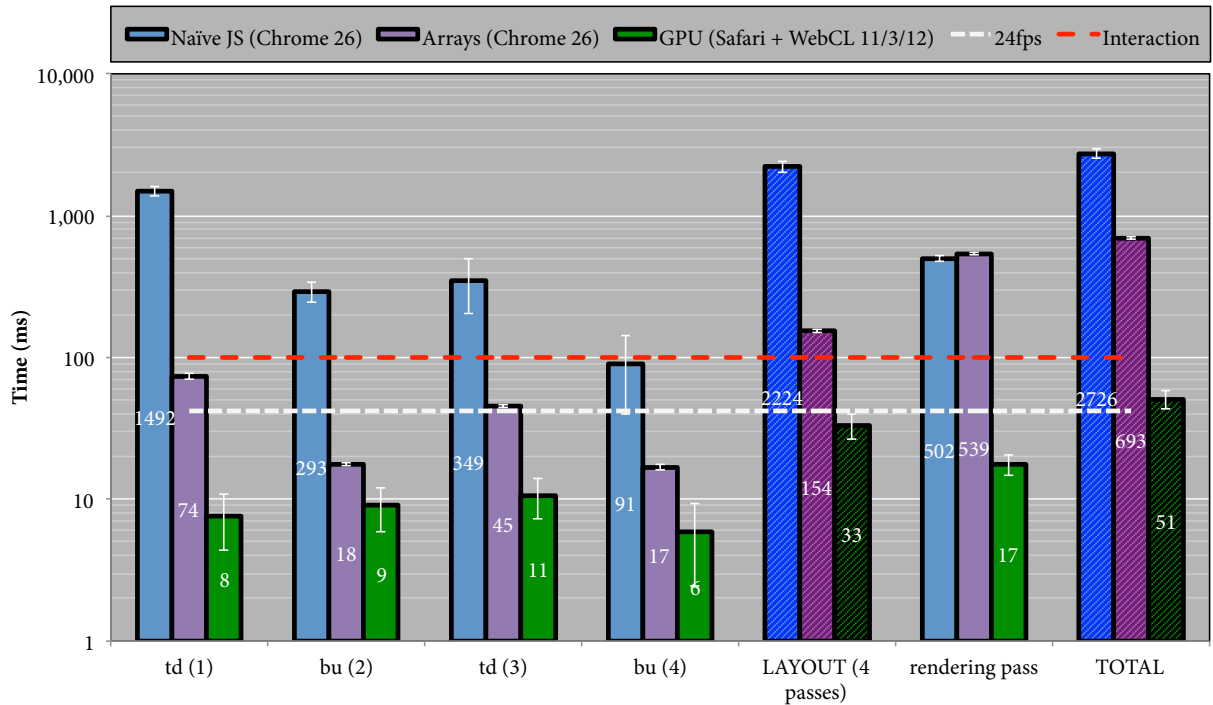


Figure 6.11: Sequential and Parallel Benefits of Breadth-First Layout and Staged Allocation. Allocation is merged into the 4th stage and buffer indexing and tessellation form the rendering pass. JavaScript variants use HTML5 canvas drawing primitives while WebCL does not include WebGL painting time (< 5ms). Thin vertical bars indicate standard deviation and horizontal bars show deadlines for animation and hand-eye interaction.

Table 6.2 shows the parallel speedup on running our 9 pass layout engine for two popular web pages that render faithfully with it: Wikipedia and the XKCD blog. Note that the benchmarks do *not* include sequential speedups. The best performance of TBB was a 1.8X speedup on 4 cores, and its speedup on 8 cores was 1.2X. In comparison, our scheduler achieved 2.8X on 2 cores and 3.2X on 8X. Our insight as to why we did not see further benefits is overheads. Across our benchmarks, we generally saw speedups when sequential traversals took longer than a certain amount, but because so many traversals are used for CSS, enough of them are small enough that we do not expect strong scaling. Our intuition is that either a full layout engine is complicated enough that the sequential cost of each traversal will be higher than in our prototype, or even more aggressive data representation optimizations should be performed. As is, we have demonstrated significant 3X+ speedups on real workloads from just the parallelization.

Baseline SIMD Speedups (GPU)

We evaluate the sequential and parallel performance benefits of our baseline breadth-first layout. For an animation to achieve 24fps, the time spent to process a frame should not exceed 42ms, and for eye-hand interactions, 100ms (10fps). We examine the case of a 5 pass treemap that supports live filtering over 100,000 data points. The first 3 passes are purely devoted to layout, the 4th pass includes layout computations and allocation requests, and the 5th pass propagates buffer indices and performs tessellation.

We compare 3 backends for our compiler: canonical JavaScript (a tree of nodes), JavaScript over our structure-split breadth-first tree layout (and with typed arrays [[CITE]]), and WebCL for the GPU. The first two variants invoke HTML5 canvas drawing primitives, while the last invokes WebGL (GPU) painting primitives over vertex buffers computed in the rendering pass. The time for WebGL painting calls are not shown, but they take less than 5ms. Each variant is repeated 15 times on a 4 core 2012 2.66GHz Intel Core i7 with 8 GB memory and a 1024 MB NVIDIA GeForce GT 650M graphics card.

We first examine the significant sequential benefits. The first 4 groups of columns in Figure 6.11 shows the average time spent on different layout passes and the 6th on the pass for buffer index computation and tessellation. Performing compiler optimizations enables a 14X sequential speedup on layout in the Chrome web browser. No speedup is observed in the rendering pass because the time is dominated by HTML5 canvas calls. We hypothesize part of the sequential benefit is related to our clustering optimization: all of the nodes in a level have the same type, so implicit optimizations such as branch prediction should perform better. Finally, we note that while sequential layout time is a magnitude too slow for real-time animation, our prototype is within 54ms for real-time interaction (ignoring rendering).

Parallel speedups are also significant. WebCL (GPU) evaluation of layout is 5X faster than sequential. The impact of compiling JavaScript vs. C (WebCL) on the benchmark is unclear: JavaScript is generally a magnitude slower than native code, except the runtime WebCL compiler is not running at high optimization levels. The benefits for parallel computation of the buffer indices and tessellation is much more clear: the speedup is 31X.

To better understand the benefit of parallelization, we compared running the layout traversals using multicore vs. GPU acceleration (Figure 6.12) for an early prototype of the layout traversals. Both use breadth-first traversals compiled with OpenCL, except differ on the hardware target. We see that a server-grade multiprocessor (32-core AMD Opteron 2356) can outperform a laptop GPU, but the comparison is unfair in terms of power consumption. TODO compare power ratings.

Ultimately, when the sequential and parallel optimizations are combined, we see an end-to-end speedup of 54X. It is high enough such that it enables real-time animation for our data set, not just real-time user interaction.

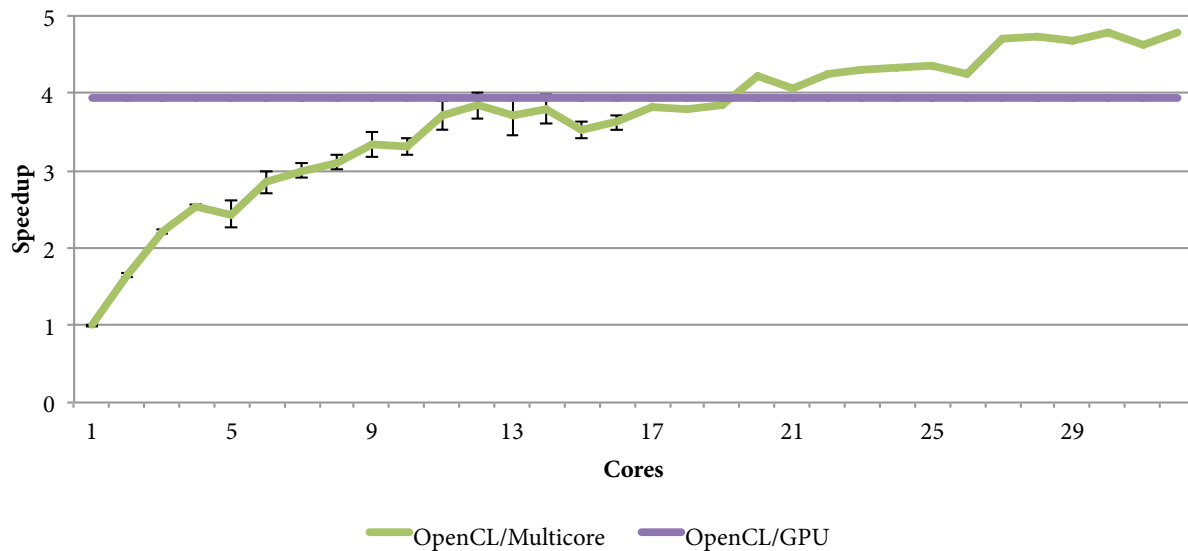


Figure 6.12: **Multicore vs. GPU Acceleration of Layout.** Benchmark on an early version of the treemap visualization and does not include rendering pass.

SIMD Clustering

We evaluate several aspects of our clustering approach. First, we examine applicability to various visualizations. Second, we evaluate the speed and performance benefit. Clustering provides invariants that benefit more than just vectorization, so we distinguish sequential vs. parallel speedups. Finally, there are different options in what clusters to form, so for each stage of evaluation, we compare impact.

Applicability

We examined idealized speedup for several workloads:

- **Synthetic.** For a controlled synthetic benchmark, we simulated the effect of increasing number of clusters on speedup for various SIMD architectures. Our simulation assumes perfect speedups for SIMD evaluation of nodes run together on a SIMD unit. The ideal speedup is a function of the minimum of the SIMD unit's length (for longer clusters, multiple SIMD invocations are mandatory) and the number of clusters (at least one SIMD step is necessary for each cluster). Figure 6.8 shows, for architectures of different vector length, that the simulated speedup from clustering (solid black line with circles) is close to the ideal speedup (solid green line).
- **Data visualization.** For our data visualizations, we found that, across the board, all of the nodes of a level shared the same type. For example, our visualization for

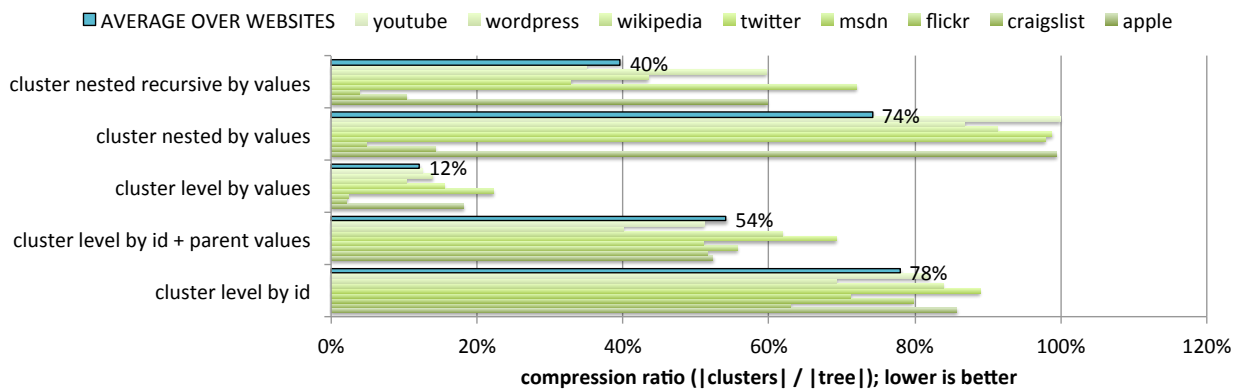


Figure 6.13: **Compression ratio for different CSS clusterings.** Bars depict compression ratio (number of clusters over number of nodes). Recursive clustering is for the reduce pattern, level-only for the map pattern. ID is an identifier set by the C3 browser for nodes sharing the same style parse information while value is by clustering on actual style field values.

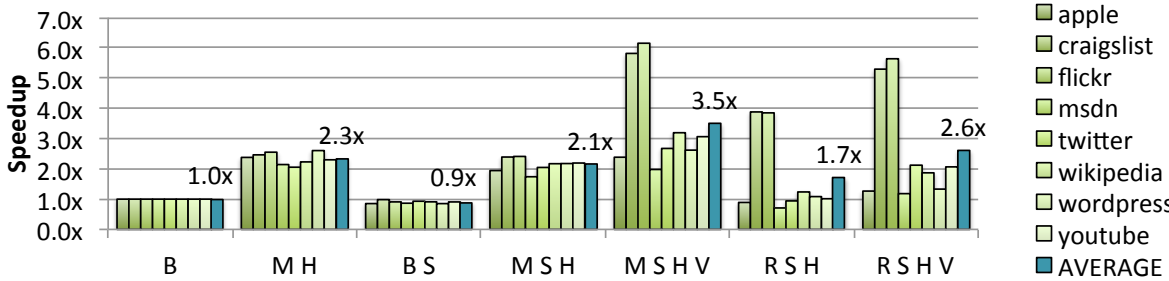
multiple line graphs puts the root node on the first level, the axis for each line graph on the second level, and all of the actual line segments on the third level.

- **CSS.** We analyzed potential speedup on webpages. Webpages are a challenging case because an individual webpage features high visual diversity, with popular sites using an average of 27KB of style data per page.¹ We picked 10 popular websites from the Alexa Top 100 US websites that rendered sufficiently correctly in the C3 [[CITE]] web browser. It was also challenging in practice because it required clustering based on individual node attributes, not just the node type.

Figure fig:csscompression compares how well nodes of a webpage can be clustered. It reports the *compression ratio*, which divides the number of clusters by the number of nodes. Sequential execution would assign each node to its own cluster, so the ratio would be 1. In contrast, if the tree is actually a list of 100 elements, and the list can be split into 25 clusters, the ratio would be 25%. Assuming infinite-length vector processors and constant-time evaluation of a node, the compression ratio is the exact inverse of the speedup. A ratio of 1 leads to a 1X speedup, and a compression ratio of 25% leads to a 4X speedup.

Clustering each level by attributes that influence control flow achieved a 12% compression ratio (Figure fig:csscompression): an 8.3X idealized speedup. When we strengthened the clustering condition to enforce stronger invariants in the cluster, such as to consider properties of the parent node, the ratio quickly worsened. Thus, we see that our basic approach is promising for websites on modern subword-SIMD instruction

¹<https://developers.google.com/speed/articles/web-metrics>



B =breadth first, S = structure splitting, M = level clustering, R = nested clustering, H = hoisting, V = SSE 4.2

Figure 6.14: **Speedups from clustering on webpage layout.** Run on a 2.66GHz Intel Core i7 (GCC 4.5.3 with flags -O3 -combine -msse4.2) and does not preprocessing time.

sets, such as a 4-wide SSE (x86) and NEON (ARM), and the more recent 8-wide AVX (x86). Even longer vector lengths are still beneficial because some clusters were long. However, eliminating all divergences requires addressing control flows influenced by attributes of node neighbors, which leads to poor compression ratios. Thus, we emphasize that 8.3X is an upper bound on the idealized speedup: not all branches in a cluster are addressed.

Empirically, we see that clustering is applicable to CSS, and in the case of our data visualizations, unnecessary. Vectorization limit studies based on analyzing dynamic data dependencies from program traces suggest that general programs can be much more aggressively vectorized, so clustering may be the beginning of one such approach [[CITE]].

Speedup

We evaluate the speedup benefits of clustering for webpage layout. We take care to distinguish sequential benefits from parallel, and of different clustering approaches. Our implementation was manual: we examine optimizing one pass of the C3 [[CITE]] browser’s CSS layout engine that is responsible for computing intrinsic dimensions. The C3 browser was written in C#, so we wrote our optimized traversal in C and pinned the memory for shared access. We use a breadth-first tree representation and schedule for our baseline, but note that doing such a layout already provides a speedup over C3’s unoptimized global layout.

For our experimental setup, we evaluate the same popular webpages above that rendered legibly with the experimental C3 browser. Benchmarks ran on a 2.66GHz Intel Core i7 (GCC 4.5.3 with flags -O3 -combine -msse4.2). We performed 1,000 trials, and to avoid warm data cache effects, iterated through different webpages.

We first examine sequential performance. Converting an array-of-structures to a structure-of-arrays causes a 10% slowdown (B S in Figure 6.14). However, clustering each level and hoisting computations shared throughout a cluster led to a 2.1X sequential benefit (M S H).

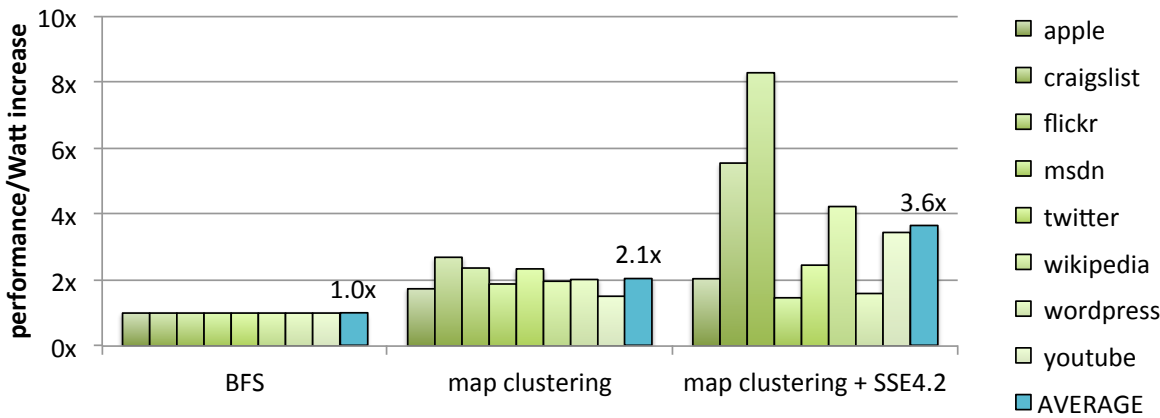


Figure 6.15: Performance/Watt increase for clustered webpage layout.

Nested clustering provided more optimization opportunities, but the compression ratio worsened: it only achieved a 1.7X sequential speedup (R S H). Clustering provides a significant sequential speedup.

Next, we examine the benefit of vectorization. SSE instructions provide 4-way SIMD parallelism. Vectorizing the nested clustering improves the speedup from 1.7X to 2.6X, and the level clustering from 2.1X to 3.5X. Thus, we see significant total speedups. The 1.7X relative speedup of vectorization, however, is still far from the 4X: level clustering suffers from randomly strided children, and the solution of nested clustering sacrifices the compression ratio.

Power

Much of our motivation for parallelization is better performance-per-Watt, so we evaluate power efficiency. To measure power, we sampled the power performance counters during layout. Each measurement looped over the same webpage over 1s due to the low resolution of the counter. Our setup introduces warm cache effects, but we argue it is still reasonable because a full layout engine would use multiple passes and therefore also have a warm cache across traversals.

In Figure 6.15, we show a 2.1X improvement in power efficiency for clustered sequential evaluation, which matches the 2.1X sequential speedup of Figure 6.14. Likewise, we report a 3.6X cumulative improvement in power efficiency when vectorization is included, which is close to the 3.5X speedup. Thus, both in sequential and parallel contexts, clustering improves performance per Watt. Furthermore, it supports the general reasoning in parallel computing of 'race-to-halt' as a strategy for improving power efficiency.

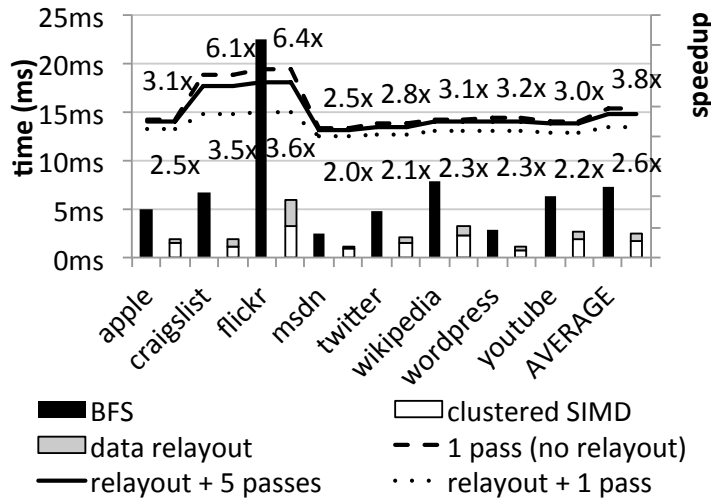


Figure 6.16: **Impact of data relayout time on total CSS speedup.** Bars depict layout pass times. Speedup lines show the impact of including clustering preprocessing time.

Overhead

Our final examination of clustering is of the overhead. Time spent clustering before layout must not outweigh the performance benefit; it is an instance of the planning problem.

For the case of data visualization, we convert the data structure into arrays with an offline preprocessor. Thus, our data visualizations experience no clustering cost.

For webpage layout, clustering is performed on the client when the webpage is received. We measured performing sequential two-pass clustering. Figure 6.16 shows the overhead relative to one pass using the bars. The highest relative overhead was for the Flickr homepage, where it reaches almost half the time of one pass. However, layout occurs in multiple passes. For a 5-pass layout engine where we model each pass as similar to the one we optimized, the overhead is amortized. The small gap between the solid and dashed lines in Figure 6.16 show there is little difference when we include the preprocessing overhead in the speedup calculation.

6.6 Related Work

1. representation The representation might be further compacted. For example, the last two arrays will have null values for Circle nodes. Even in the case of full utilization, space can be traded for time for even more aggressive compression [[CITE rinard]]
2. sims limit studies
3. duane

4. trishul
5. gnu irregular array stuff

Chapter 7

Conclusion

Appendix A

Layout Grammars